

Likelihood Level Adapted Estimation of Marginal Likelihood for Bayesian Model Selection

Subhayan De^{a,*}, Reza Farzad^b, Patrick T. Brewick^b, Erik A. Johnson^c, Steven F. Wojtkiewicz^d

^a*Department of Mechanical Engineering, Northern Arizona University, Flagstaff, AZ 86011, USA*

^b*Department of Civil and Environmental Engineering & Earth Sciences, University of Notre Dame, IN 46556, USA*

^c*Sonny Astani Department of Civil and Environmental Engineering, University of Southern California, Los Angeles, CA 90089, USA*

^d*Department of Civil and Environmental Engineering, Clarkson University, Potsdam, NY 13699, USA*

Abstract

In computational mechanics, multiple models are often present to describe a physical system. While Bayesian model selection is a helpful tool to compare these models using measurement data, it requires the computationally expensive estimation of a multidimensional integral — known as the marginal likelihood or as the model evidence (*i.e.*, the probability of observing the measured data given the model) — over the multidimensional parameter domain. This study presents efficient approaches for estimating this marginal likelihood by transforming it into a one-dimensional integral that is subsequently evaluated using a quadrature rule at multiple adaptively-chosen iso-likelihood contour levels. Three different algorithms are proposed to estimate the probability mass at each adapted likelihood level using samples from importance sampling, stratified sampling, and Markov chain Monte Carlo sampling, respectively. The proposed approach is illustrated through four numerical examples. The first, an elementary example, shows the accuracies of the three proposed algorithms when the exact value of the marginal likelihood is known. The second example uses an 11-story building subjected to an earthquake excitation with an uncertain hysteretic base isolation layer with two models to describe the isolation layer behavior. The third example considers flow past a cylinder when the inlet velocity is uncertain. Based on these examples, the method with stratified sampling is by far the most accurate and efficient method for complex model behavior in low dimension, particularly considering that this method can be implemented to exploit parallel computation. In the fourth example, the proposed approach is applied to heat conduction in an inhomogeneous plate with uncertain thermal conductivity modeled through a 100 degree-of-freedom Karhunen-Loève expansion. The results indicate that MultiNest cannot efficiently handle the high-dimensional parameter space, whereas the proposed MCMC-based method more accurately and efficiently explores the parameter space. The marginal likelihood results for the last three examples, when compared with the results obtained from standard Monte Carlo sampling and nested sampling, show good agreement.

Keywords: Bayesian model selection, marginal likelihood, probability integral transform, Markov chain Monte Carlo.

1. Introduction

In computational mechanics, one often encounters the dilemma of choosing a model, for a physical system or phenomenon, that is computationally efficient as well as accurate. This model may be used for response prediction, design optimization, experiment design, and so forth. There are a variety of model selection criteria based on information theory representing a trade-off between model's simplicity and the fit accuracy, including but not limited to Akaike information criterion (AIC) [1], Bayesian-Schwarz information criterion (BIC) [2], the focused information criterion (FIC) [3], the minimum description length principle (MDL) [4], and the deviance information criterion (DIC) [5]. DIC has been developed concerning the prediction accuracy of future datasets rather than considering model selection and, therefore, Bayesian evidence outperforms DIC in some cases. However, two common philosophies to guide the model choice across a set of candidate models are *model falsification* [6, 7] and *model selection* [8] (it has also been shown that the model falsification is equivalent to approximate Bayesian computation (ABC) [9]). In model falsification, models are eliminated using measurement data but no relative judgement is provided among the remaining unfalsified models. On the other hand, in *Bayesian model selection*, one or more model(s) are selected from a larger candidate set [10–13] by ranking them based on posterior model probabilities; however, to estimate those probabilities, a multidimensional integral over the model parameter domain must be evaluated. This model selection approach has been applied to a wide range of fields, *e.g.*, finance [14], genetics [15], signal processing [16], and structural dynamics [17–21]. In Bayesian model selection [22], Bayes' theorem is applied to quantify the likelihood that each model could generate the measurement data. A common form of Bayesian model selection uses the *Bayes factor*, which is a ratio of the marginal likelihoods of, or evidences for, two models [23, 24]. Note that the *Occam's razor* principle, which suggests that models with lesser complexity should be favored among models of comparable accuracy, is also embedded in Bayesian model selection, as discussed in Beck and Yuen [17], MacKay [25, 26], and Gull [27]. A combined model selection and falsification approach can also be followed as shown in De *et al.* [11]; however, this approach still requires the estimation of marginal likelihood for a few models.

The main computational effort in Bayesian model selection arises in the accurate estimation of the *evidence*, the marginal likelihood for each model, requiring many forward model simulations. A standard Monte Carlo estimation proves costly in this case when the number of model parameters increases. A number of methods have been proposed in

*Corresponding author

Email addresses: Subhayan.De@nau.edu (Subhayan De), rfarzad@nd.edu (Reza Farzad), pbrewick@nd.edu (Patrick T. Brewick), JohnsonE@usc.edu (Erik A. Johnson), swojtkie@clarkson.edu (Steven F. Wojtkiewicz)

recent decades to intelligently select the random samples needed to estimate the marginal likelihood or evidence. For example, the posterior harmonic mean estimator [28] samples from the posterior distributions of the parameters; this estimator, however, may have infinite variance [29]. Importance sampling [23, 30] and its adaptive variants [31, 32] have also been applied to improve the efficiency of standard Monte Carlo sampling to estimate the marginal likelihood. Annealed importance sampling [33, 34] and the power posterior method [35] are closely related to thermodynamic integration and may also be used. Ching *et al.* [36] introduced the Transitional Markov Chain Monte Carlo method in which samples, drawn from intermediate distributions, ultimately converge to a target distribution, providing an estimate of the marginal likelihood. Similarly, subset simulation methods [37–40] and polynomial chaos approaches [41] may also be employed to estimate the marginal likelihood; however, the estimates provided by these methods can be biased as they are prone to using correlated random samples or approximated likelihood functions.

Skilling [42] proposed a method for the estimation of marginal likelihood that converts the multi-dimensional marginal likelihood integral into a one-dimensional integral representation. This method, known as nested sampling, simplifies the integration task, but requires more samples from the high-likelihood region. MultiNest is a widely-used algorithm for efficient implementation of nested sampling for multi-modal posteriors [43, 44]. Considering the same mechanism used by MultiNest, Feroz *et al.* [45] presented the more efficient importance nested sampling method by using previously discarded samples. Polson and Scott [46] outlined an approach, namely “vertical-likelihood Monte Carlo,” based on a Lebesgue representation of the marginal likelihood that unifies nested sampling and other developments for marginal likelihood estimation; however, evaluating the resulting converted one-dimensional integral is not straightforward and incurs exorbitant computational costs for large-scale complex models with high-dimensional uncertainty. Therefore, with the advent of newer and more complex models to elaborate system behavior in greater depth, there is a need for novel and enhanced methods to efficiently explore stochastic parameter spaces in higher dimensions. Readers are referred to Llorente *et al.* [47] for an extensive and up-to-date review of marginal likelihood computation for model selection, including detailed descriptions, advantages, and weaknesses.

Herein, an adaptive approach is proposed to estimate the marginal likelihood. In this proposed approach, a probability integral transformation is first used to convert the multidimensional integration of marginal likelihood into a one-dimensional integration in a similar approach to the “vertical-likelihood Monte Carlo” [46]. The resulting one-dimensional integral is then evaluated using a quadrature rule; the quadrature points are calculated using an adaptive likelihood level approach, where samples with increasing levels of likelihoods are sequentially generated. Three algorithms to efficiently generate these random samples — based on importance sampling, stratified sampling, and Markov chain Monte Carlo sampling, respectively — are presented herein. In the first algorithm, samples for the current likelihood level are generated from an importance distribution formed using the samples from previous levels. In the second proposed algorithm, a subset of strata that contains samples from the previous level are used to generate samples for the current likelihood level. In the third algorithm, Markov chains are run starting from the previous level’s samples to

generate samples for the current likelihood level. The proposed algorithms provide flexibility in choosing the likelihood levels to focus on regions with high likelihood values, thereby providing better computational efficiency relative to standard Monte Carlo sampling. Further, samples from posterior model parameter distribution are not needed for the estimation; additionally, moments of the posterior distribution are generated as by product of these algorithms.

The proposed algorithms are illustrated using four numerical examples. First, an elementary example with a Gaussian likelihood and a Gaussian prior is used so that the true value of the evidence or marginal likelihood is known and accuracies can be assessed. Note that the terms evidence and marginal likelihood are used interchangeably herein. The second example studies an 11-story base-isolated building with uncertainty in the nonlinear hysteretic isolation layer. Using roof acceleration measurements, the evidence or marginal likelihood is estimated for a linear approximation of the isolation layer and for two nonlinear model classes, namely, Bouc-Wen and bilinear hysteresis models. A comparison with Monte Carlo, nested sampling, and MultiNest is used to evaluate the results computed with the proposed approach. In the third example, velocities of a two-dimensional flow are measured at several points downstream from a cylinder in a closed channel. The inlet velocity profile is assumed to be parabolic with an uncertain maximum inlet velocity distributed as a truncated Gaussian. The marginal likelihood of the fluid flow model using the discretized Navier-Stokes equation and uncertain inlet velocity is computed using the proposed algorithms and again compared with that from Monte Carlo and nested sampling. In the final example, an inhomogeneous plate with uncertain thermal conductivity is used to illustrate one of the proposed algorithms. The thermal conductivity is expressed using a random field represented by a Karhunen-Loeve expansion. This example has a parameter space that is of significantly higher dimension compared to the previous three examples. The results show close agreement with Monte Carlo and nested sampling.

This paper is organized as follows. The next section provides brief backgrounds of Bayesian model selection and various sampling strategies. The three proposed algorithms are presented in Section 3 with a discussion of issues related to their implementation in Section 4. Then, in Section 5, four numerical examples are used to illustrate the proposed algorithms, followed by conclusions in Section 6.

2. Background

2.1. Definition of a Model

A model to represent some physical phenomenon is defined here by a set of mathematical equations. Based on the characteristics of these equations, a model may be linear or nonlinear, and may describe static or dynamic behavior. The k th model is parameterized by a set of parameters $\boldsymbol{\theta}_k \in \mathbb{R}^{n_{\theta_k}}$ (the model number k will be omitted subsequently for notational simplicity).

2.2. Bayesian Model Selection

Let $\mathcal{M} = \{\mathcal{M}_1, \mathcal{M}_2, \dots, \mathcal{M}_{N_{\mathcal{M}}}\}$ be the set of $N_{\mathcal{M}}$ different models considered to describe a particular system. Given a data set \mathfrak{D} containing measurements from the physical system,

the goal of Bayesian model selection is to select the most plausible model(s) to represent the system. The *posterior* model probabilities (*i.e.*, the probability of each model conditioned on measurement data \mathfrak{D}) are given by Bayes' theorem:

$$\mathbb{P}(\mathcal{M}_k|\mathfrak{D}) = \frac{p(\mathfrak{D}|\mathcal{M}_k)\mathbb{P}(\mathcal{M}_k)}{p(\mathfrak{D})}, \quad k = 1, 2, \dots, N_{\mathcal{M}}. \quad (1)$$

where $\mathbb{P}(\mathcal{M}_k)$ is an *a priori* measure of model plausibility assigned by the modeler based on past experience, normalized so $\sum_{k=1}^{N_{\mathcal{M}}} \mathbb{P}(\mathcal{M}_k) = 1$, and denominator

$$p(\mathfrak{D}) = \sum_{k=1}^{N_{\mathcal{M}}} p(\mathfrak{D}|\mathcal{M}_k)\mathbb{P}(\mathcal{M}_k) \quad (2)$$

using the theorem of total probability. Herein, $\mathbb{P}(\cdot)$ denotes a probability; $p(\cdot)$ denotes a probability density and the notation $\theta_j \sim p(\theta)$ denotes choosing a sample θ_j according to the density $p(\theta)$.

For a particular model \mathcal{M}_k , the model evidence or marginal likelihood $\mathcal{E}^{(k)} = p(\mathfrak{D}|\mathcal{M}_k)$ is

$$\begin{aligned} \mathcal{E}^{(k)} &= \int_{\Theta} p(\mathfrak{D}|\theta, \mathcal{M}_k)p(\theta|\mathcal{M}_k)d\theta \\ &= \int_{\Theta} \mathcal{L}(\theta, \mathcal{M}_k)p(\theta|\mathcal{M}_k)d\theta \end{aligned} \quad (3)$$

where $\theta \in \Theta$ is the (uncertain) parameter vector, with prior probability $p(\theta|\mathcal{M}_k)$ for model \mathcal{M}_k , and $\mathcal{L}(\theta, \mathcal{M}_k) = p(\mathfrak{D}|\theta, \mathcal{M}_k)$ is the likelihood function (*i.e.*, the data likelihood given a model and parameter vector). (It is assumed herein that the data are continuous quantities, but the approach can be adapted for discrete quantities by replacing densities $p(\cdot)$ with probabilities $\mathbb{P}(\cdot)$; mixed continuous/discrete quantities can be accommodated as long as either the likelihood $\mathcal{L}(\theta, \mathcal{M}_k)$ or the parameter prior $p(\theta|\mathcal{M}_k)$ are finite for all $\theta \in \Theta$.)

2.3. Evidence Computation via Nested Sampling

As shown in (3), computing the model evidence (marginal likelihood) $\mathcal{E}^{(k)}$ is more computationally demanding for models with a greater number of parameters, since it requires computing the high-dimensional integral over the entire domain of parameter space. Nested sampling was introduced by Skilling [42] to convert the evaluation of the evidence into a tractable one-dimensional integral. While this has proven to be a powerful technique, the underlying method still relies upon Monte Carlo sampling, which is poorly suited to multi-modal parameter spaces. To address this challenge, Shaw *et al.* [48] proposed a clustered nested sampling method to form multiple ellipsoidal clusters to capture multi-modal posterior distributions. The MultiNest algorithm was subsequently developed [49] and improved [43] by Feroz *et al.* as a more advanced means of simultaneous ellipsoidal nested sampling. A brief review of the MultiNest algorithm is presented below; for complete details, the interested reader should consult Feroz *et al.* [43].

The MultiNest method is initialized by selecting N_{live} active points by randomly sampling over the entire parameter space. To account for the multi-modality, MultiNest assigns active points to clusters (groups) bounded by iso-likelihood contours. A series of (possibly overlapping) ellipsoids are then simultaneously formed and bounded around each cluster of active points. The optimal ellipsoidal decomposition of active points is performed using an “expectation-maximization” approach to minimize the total volume V_{tot} of the ellipsoids while satisfying $V_{\text{tot}} > X_i/f$, where $X_i \approx \exp(-i/N_{\text{live}})$ is the expected prior volume, and $0 < f < 1$ is a user-defined value for the target efficiency. As f increases, the minimum total volume decreases, and the EM algorithm chooses smaller V_{tot} , leading to faster algorithm convergence, but at the possible cost that the algorithm might not cover the full likelihood volume, resulting in biased estimates. Another issue is the possibility of an overshoot of the ellipsoidal decomposition in higher dimensions, leading to a remarkable decrease in sampling efficiency.

After constructing the ellipsoidal bounds, new samples are generated uniformly from within the bounded ellipsoids. More specifically, the probability of choosing ellipsoid l among L ellipsoids is V_l/V_{tot} , in which $V_{\text{tot}} = \sum_{l=1}^L V_l$. Then, if a new sample has a larger likelihood value than the minimum likelihood within the active points, *i.e.*, $\mathcal{L}_{\text{new}} > \mathcal{L}_{\text{min}}$, the newly drawn sample is accepted to replace the minimum likelihood value with probability $1/q$, where q is the number of ellipsoids containing the point. This process reduces the possibility of sampling too many points from highly-intersected regions, leading to proper sampling from all ellipsoids.

Using the updated set of active points, another set of ellipsoids is formed and new samples are generated to replace the new minimum likelihood value(s). This iterative process continues until some convergence criterion is satisfied, *e.g.*, a maximum number of iterations or a tolerance related to the evidence evaluation. The advantage of MultiNest is that it is flexible enough to explore a range of complicated posterior shapes through constructing non-overlapping and overlapping ellipsoids. In this study, the target efficiency parameter f , representing the fraction of the expected prior volume enclosed by the ellipsoidal bounds, is fixed at 10%. The only hyper-parameter set for each application is the number of active points, which is specified for each application.

2.4. Review of Sampling Methods

The proposed algorithm will use three sampling methods, which are reviewed in this section assuming, for notational simplicity, a scalar parameter $\theta \in \Theta$.

2.4.1. Importance sampling

Importance sampling is used to estimate an expectation $\mu_f = \mathbb{E}_p[f(\theta)]$ when sampling from the density $p(\theta)$ is difficult [50]. Importance sampling instead draws N samples $\{\theta_j\}_{j=1}^N$ from a similar density function $q(\theta)$, called the importance sampling density (ISD), and gives the unbiased estimate as

$$\hat{\mu}_f^{\text{IS}} = \frac{1}{N} \sum_{j=1}^N f(\theta_j) w_j \quad (4)$$

where the *importance weights* $w_j = p(\theta_j)/q(\theta_j)$ are used to correct the bias introduced by sampling from $q(\theta)$. The variance of the estimator is given by

$$\text{Var}_q [\hat{\mu}_f^{\text{IS}}] = \frac{1}{N} \left\{ \mathbb{E}_p \left[f^2(\theta) \frac{p(\theta)}{q(\theta)} \right] - \mu_f^2 \right\} \quad (5)$$

The reduction in variance obtained compared to a standard Monte Carlo estimator $\hat{\mu}_f^{\text{MC}} = \frac{1}{N} \sum_{j=1}^N f(\theta_j)$ with $\theta_j \sim p(\theta)$ is given by

$$\text{Var}_p [\hat{\mu}_f^{\text{MC}}] - \text{Var}_q [\hat{\mu}_f^{\text{IS}}] = \frac{1}{N} \left\{ \mathbb{E}_p \left[f(\theta)^2 \left(1 - \frac{p(\theta)}{q(\theta)} \right) \right] \right\} \quad (6)$$

Hence, the use of importance sampling can produce variance reduction by choosing the importance density proportional to $|f(\theta)|p(\theta)$. However, $p(\theta)$ or $q(\theta)$ are often known up to a constant. In that case, one may use a normalized importance sampling (NIS), which estimates the expectation as

$$\hat{\mu}_f^{\text{NIS}} = \sum_{j=1}^N f(\theta_j) \tilde{w}_j \quad (7)$$

where the normalized weights \tilde{w}_j are given by

$$\tilde{w}_j = \frac{w_j}{\sum_{i=1}^N w_i} = \frac{p(\theta_j)/q(\theta_j)}{\sum_{i=1}^N p(\theta_i)/q(\theta_i)} \quad (8)$$

This normalized importance sampling estimator is biased but consistent (*i.e.*, asymptotically unbiased). Choosing $q(\theta) > 0$ whenever $p(\theta) > 0$ also achieves variance reduction. A measure of effectiveness in using the importance density $q(\theta)$, the effective sample size (ESS), is given by

$$\text{ESS} = \frac{\left(\sum_{j=1}^N w_j \right)^2}{\sum_{j=1}^N w_j^2} \quad (9)$$

2.4.2. Stratified sampling

Stratified sampling suggests dividing the sample space Θ into \bar{n}_{st} disjoint subspaces $\{\Theta^{(s)}\}_{s=1}^{\bar{n}_{\text{st}}}$ where $\cup_{s=1}^{\bar{n}_{\text{st}}} \Theta^{(s)} = \Theta$ and $\Theta^{(r)} \cap \Theta^{(s)} = \emptyset$ for $r \neq s$. The mean of the quantity f is then estimated within each of these strata, denoted as $\hat{\mu}_f^{(s)}$ for $s = 1, \dots, \bar{n}_{\text{st}}$. The strata means are then combined, using the theorem of total probability, to give

$$\mathbb{E}_p[f] \approx \hat{\mu}_f^{\text{SS}} = \sum_{s=1}^{\bar{n}_{\text{st}}} \hat{\mu}_f^{(s)} p^{(s)} \quad (10)$$

where $p^{(s)} = \mathbb{P}(\Theta^{(s)})$. The variance reduction compared to the standard Monte Carlo method is given by McKay *et al.* [51]

$$\text{Var}_{\mathbb{P}} [\hat{\mu}_f^{\text{MC}}] - \text{Var}_{\mathbb{P}|\Theta} [\hat{\mu}_f^{\text{SS}}] = \frac{1}{N} \sum_{s=1}^{\bar{n}_{\text{st}}} (\hat{\mu}_f^{(s)} - \hat{\mu}_f^{\text{SS}})^2 p^{(s)} \quad (11)$$

where each strata mean $\hat{\mu}_f^{(s)}$ is calculated using $N^{(s)} = p^{(s)}N$ samples for $s = 1, \dots, \bar{n}_{\text{st}}$.

2.4.3. Markov chain Monte Carlo (MCMC)

Markov chain Monte Carlo is used to sample from a distribution otherwise difficult to sample [52, 53]. For this purpose, a Markov chain with stationary distribution $\pi(\cdot)$ is constructed to explore the sample space Θ and choose samples [54]. The invariant distribution of the chain satisfies

$$\pi(\eta)d\eta = \int_{\Theta} K(\theta, d\eta)\pi(\theta)d\theta \quad (12)$$

where the transition kernel of the Markov chain is defined as [52, 55]

$$K(\theta, d\eta) = f(\theta, \eta)d\eta + \left[1 - \int_{\Theta} f(\theta, \eta)d\eta\right] \delta_{\theta}(d\eta) \quad (13)$$

for some transition function $f(\theta, \eta)$ with conditions that $f(\theta, \theta) = 0$ and $\delta_{\theta}(d\eta) = 1$ for $\theta \in d\eta$ or 0 for $\theta \notin d\eta$. The probability of the chain staying at θ is $[1 - \int_{\Theta} f(\theta, \eta)d\eta]$. A popular algorithm for generating samples using MCMC is the *Metropolis-Hastings (MH) algorithm*, which assumes that the transition from θ to η , for $\theta \neq \eta$, is of the form [52]

$$f_{\text{MH}}(\theta, \eta) = q(\theta, \eta)\alpha(\theta, \eta) \quad (14)$$

where $q(\theta, \eta)$ is an assumed proposal density and $\alpha(\theta, \eta)$ is the acceptance rate defined by

$$\alpha(\theta, \eta) = \begin{cases} \min \left[\frac{\pi(\eta)q(\eta, \theta)}{\pi(\theta)q(\theta, \eta)}, 1 \right], & \text{for } \pi(\theta)q(\theta, \eta) > 0 \\ 1, & \text{for } \pi(\theta)q(\theta, \eta) = 0 \end{cases} \quad (15)$$

However, with increasing dimension, the MH algorithm becomes inefficient. Au and Beck [56] proposed a modified algorithm, used in the numerical examples herein, with a higher acceptance of generated candidate samples by using the MH algorithm component-wise.

3. Proposed Methodology

3.1. Probability integral transform

Evidence integral (3), omitting model variable \mathcal{M}_k , is rewritten in (16) by:

- (i) expressing the likelihood $\mathcal{L}(\boldsymbol{\theta}) = \int_0^{\mathcal{L}(\boldsymbol{\theta})} d\lambda$;
- (ii) rearranging the order of integration;

- (iii) defining a monotonically nonincreasing function $\chi(\lambda)$ that is the probability mass enclosed in the parameter space subset where likelihoods $\mathcal{L}(\boldsymbol{\theta})$ exceed λ ;
- (iv) defining the monotonically nonincreasing inverse function $\varphi(\chi)$, the likelihood level that contains a given probability mass; *i.e.*, $\varphi(\chi(\lambda)) \equiv \lambda$;
- (v) changing the variable of integration;
- (vi) approximating the integral by discretizing over χ ; and
- (vii) defining $\varphi_i = \varphi(\chi_i) \equiv \lambda_i$.

$$\begin{aligned}
\mathcal{E} &= \int_{\Theta} p(\mathfrak{D}|\boldsymbol{\theta})p(\boldsymbol{\theta})d\boldsymbol{\theta} \\
&= \int_{\Theta} \mathcal{L}(\boldsymbol{\theta})p(\boldsymbol{\theta})d\boldsymbol{\theta} \\
&= \int_{\Theta} \underbrace{\left[\int_0^{\mathcal{L}(\boldsymbol{\theta})} d\lambda \right]}_{\mathcal{L}(\boldsymbol{\theta})} p(\boldsymbol{\theta})d\boldsymbol{\theta} \\
&= \int_0^\infty \underbrace{\left[\int_{\mathcal{L}(\boldsymbol{\theta})>\lambda} p(\boldsymbol{\theta})d\boldsymbol{\theta} \right]}_{\chi(\lambda)} d\lambda \\
&= \int_0^\infty \chi(\lambda)d\lambda = \int_0^1 \varphi(\chi)d\chi \approx \sum_{i=1}^{i_{\text{final}}} \varphi_i \Delta\chi_i = \sum_{i=1}^{i_{\text{final}}} \lambda_i \Delta\chi_i
\end{aligned} \tag{16}$$

Once the multidimensional integral is converted into a one-dimensional integral, the problem becomes estimation of χ_i for a corresponding $\varphi_i \equiv \lambda_i$. Figure 1 shows that the samples from successive likelihood levels are used to convert to (λ, χ) coordinates to estimate the integral using a quadrature rule. Note that the authors previously showed [10] that the transformation (16) is also the backbone of the nested sampling method [42].

For efficient estimation of the χ_i to perform the quadrature, different variance reduction methods can be implemented; three such algorithms are proposed in the remainder of this section. Each algorithm is iterative with common stopping criteria that will be discussed in Section 4.2. Additionally, the iterations begin with a low likelihood λ_0 close to zero and advance to greater likelihood levels $\lambda_i > \lambda_{i-1}$, as discussed in Section 4.4.

3.2. Likelihood level adapted importance sampling (LLA-IS)

The first method employs importance sampling to estimate χ_i , which can be written

$$\chi_i = \mathbb{P}(\boldsymbol{\theta} \in \tilde{\Theta}_i) = \mathbb{E} [\mathbb{I}_{\tilde{\Theta}_i}(\boldsymbol{\theta})] \tag{17}$$

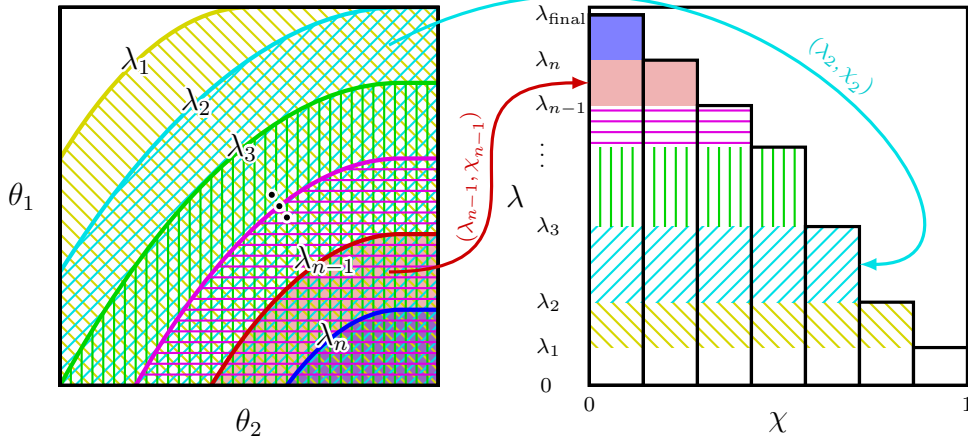


Figure 1: Likelihood level adapted estimation of marginal likelihood. Note that, $\lambda_1 < \lambda_2 < \dots < \lambda_{n-1} < \lambda_n$.

where the parameter domain $\tilde{\Theta}_i$ is the region in which the likelihood is above λ_i , *i.e.*,

$$\tilde{\Theta}_i = \{\boldsymbol{\theta} | \mathcal{L}(\boldsymbol{\theta}) > \lambda_i, \boldsymbol{\theta} \in \Theta\} \quad (18)$$

for positive integer $i \in \mathbb{Z}^+$, and where the indicator function $\mathbb{I}_{(\cdot)}(\cdot)$ is defined by

$$\mathbb{I}_{\tilde{\Theta}_i}(\boldsymbol{\theta}) = \begin{cases} 1 & \text{if } \boldsymbol{\theta} \in \tilde{\Theta}_i \\ 0 & \text{otherwise} \end{cases} \quad (19)$$

Hence, the quantity χ_i in (17) can be approximated with the estimator

$$\hat{\chi}_i^{\text{IS}} = \frac{1}{N} \sum_{j=1}^N \mathbb{I}_{\tilde{\Theta}_i}(\boldsymbol{\theta}_{j,i}) w_{j,i} \quad (20)$$

where $w_{j,i} = p(\boldsymbol{\theta}_{j,i})/q(\boldsymbol{\theta}_{j,i})$; $q(\cdot)$ is the importance sampling density with $q(\boldsymbol{\theta}) > 0$ whenever $p(\boldsymbol{\theta}) > 0$. The importance density $q(\boldsymbol{\theta})$ can be chosen as a normal distribution with mean at the posterior mode $\hat{\boldsymbol{\theta}}$ guessed from the previous set of samples and arbitrarily large variance $\hat{\Sigma}$ [57]. A threshold γ_S for effective sample size is chosen beforehand. For example, with $\gamma_S = 0.5N$, more random samples are added if the effective sample size falls below 50% of N . A large threshold γ_S increases the computational budget as new random samples are more often added to the sample pool; a small γ_S , on the other hand, will lead to slow convergence. In this paper, $\gamma_S = 0.5N$ is used. The choice of λ_i is, however, made after the simulation of N samples for practicality. The main challenge applying this algorithm lies in choosing the appropriate form for the importance densities. The spread of the importance densities

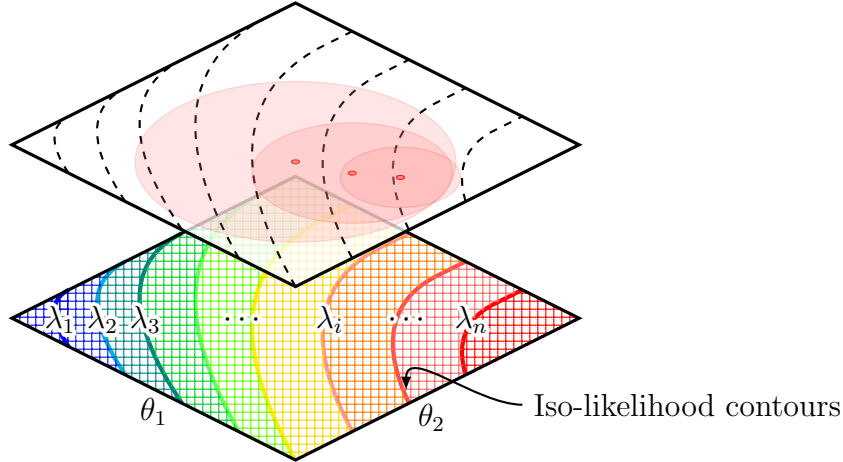


Figure 2: Likelihood level adapted importance sampling (LLA-IS) method: the iso-likelihood contours are shown with $\lambda_1 < \lambda_2 < \dots < \lambda_n$; importance densities are formed successively to generate samples from high likelihood region.

should be chosen carefully as a small spread can result in an erroneous estimation whereas a large spread will result in a slow or non-convergence. Herein, Gaussian probability densities are used for the importance densities. The means of these Gaussian densities are fixed at the means of the retained samples and the standard deviations as twice the standard deviations estimated using the retained samples. Note that finding a good importance sampling density in high-dimensional spaces can become increasingly difficult and computationally expensive as well. An algorithm for likelihood level adapted estimation of marginal likelihood (evidence) using importance sampling is presented in Algorithm 1. The algorithm starts with $\hat{\chi}_0^{\text{IS}} = 1$ and a small λ_0 that is very small or equal to zero. The importance density at the start is same as the parameter prior. The algorithm chooses likelihood threshold λ_i , greater than λ_{i-1} in the previous iteration, and estimates the corresponding $\hat{\chi}_i^{\text{IS}}$ using the importance weight as shown in (20). At the end of every iteration, the evidence is updated using a quadrature rule (the algorithms herein use a rectangular quadrature, though they could be easily adapted toward higher-order schemes). If the effective sample size falls below the pre-chosen threshold γ_S , additional samples are drawn from the current importance density. In Figure 2, the increasing likelihood contours as well as a schematic of importance densities formed near the high-likelihood region are shown as the algorithm progresses.

Algorithm 1: Likelihood level adapted marginal likelihood estimation using importance sampling (LLA-IS).

```

1 Initialization: Set  $\widehat{\chi}_0^{\text{IS}} = 1$ ,  $\widehat{\mathcal{E}}_0^{\text{IS}} = 0$ ,  $q_0(\cdot) = p(\cdot)$ , and  $\lambda_0 = 0$ ; choose a suitable  $\gamma_S$ 
   based on a computational budget (e.g.,  $\gamma_S = 0.5N$ )
2 Set  $i = 1$ 
3 while Stopping Criterion = FALSE do
4   Draw samples  $\boldsymbol{\theta}_{j,i} \sim q_{i-1}(\boldsymbol{\theta})^\dagger$  for  $j = 1, \dots, N$ 
5   Select a suitable new likelihood level  $\lambda_i > \lambda_{i-1}$  (see Section 4.4)
6   Define the likelihood exceedence region  $\widetilde{\Theta}_i = \{\boldsymbol{\theta} | \mathcal{L}(\boldsymbol{\theta}) > \lambda_i, \boldsymbol{\theta} \in \Theta\}$ 
7   Calculate likelihood values  $\mathcal{L}(\boldsymbol{\theta}_{j,i})$ ,  $j = 1, \dots, N$ , for these samples
8   Evaluate the importance weights  $w_{j,i} = p(\boldsymbol{\theta}_{j,i})/q_i(\boldsymbol{\theta}_{j,i})$ ,  $j = 1, \dots, N$ 
9   if  $\text{ESS} = \left(\sum_{j=1}^N w_{j,i}\right)^2 / \sum_{j=1}^N w_{j,i}^2 > \gamma_S$  then
10    |  $\widehat{\chi}_i^{\text{IS}} \approx \frac{1}{N} \sum_{j=1}^N \mathbb{I}_{\widetilde{\Theta}_i}(\boldsymbol{\theta}) w_{j,i}$ 
11  else
12    | Draw another  $\lceil \gamma_S - \text{ESS} \rceil$  samples from density  $q_i(\boldsymbol{\theta})$ 
13    | Go to line 7
14  Update the marginal likelihood  $\widehat{\mathcal{E}}_i^{\text{IS}} = \widehat{\mathcal{E}}_{i-1}^{\text{IS}} + \lambda_i (\widehat{\chi}_{i-1}^{\text{IS}} - \widehat{\chi}_i^{\text{IS}})$ 
15  Assume† a proper importance density  $q_i(\cdot)$  based on the samples  $\boldsymbol{\theta}_{1,i}, \dots, \boldsymbol{\theta}_{N,i}$ 
   from this iteration
16   $i \leftarrow i + 1$ 

```

Result: The marginal likelihood $\widehat{\mathcal{E}}_{\text{final}}^{\text{IS}}$

[†] Herein, for $i \geq 1$, a Gaussian distribution is assumed for $q_i(\cdot)$, with a mean the same as the mean of the samples with $\mathcal{L}(\boldsymbol{\theta}_{j,i}) > \lambda_i$ and a standard deviation twice the standard deviations estimated using the retained samples as discussed in Section 3.2.

3.3. Likelihood level adapted stratified sampling (LLA-SS)

The second algorithm proposed here implements stratified sampling in the likelihood level adapted approach, estimating $\mathbb{P}(\boldsymbol{\theta} \in \tilde{\Theta}_i)$ by focusing on the strata where at least one sample $\boldsymbol{\theta}_{j,i}$ has $\mathcal{L}(\boldsymbol{\theta}_{j,i}) > \lambda_i$. Figure 3 shows a hypothetical set of strata, highlighting those containing at least one sample with likelihood greater than some level λ_i .

Let the sample space Θ be divided into $\bar{n}_{\text{st}} = (n_{\text{st}})^{n_{\boldsymbol{\theta}}}$ disjoint strata $\Theta^{(1)}, \Theta^{(2)}, \dots, \Theta^{(\bar{n}_{\text{st}})}$ such that $\cup_{s=1}^{\bar{n}_{\text{st}}} \Theta^{(s)} = \Theta$ and $\Theta^{(r)} \cap \Theta^{(s)} = \emptyset$ for $r \neq s$. In iteration i , which will target samples whose likelihoods exceed a level λ_i , samples will only be drawn from the subset of strata, denoted by the strata index set \mathcal{I}_{i-1} , that contained one or more samples with likelihoods exceeding the likelihood level λ_{i-1} during the previous iteration ($i-1$); for the first iteration, \mathcal{I}_0 contains the indices of all strata. A new likelihood level λ_i is chosen larger than the previous λ_{i-1} (e.g., $\lambda_i = 10^\alpha \lambda_{i-1}$ for some $\alpha > 0$). In each stratum s , draw $N_i^{(s)}$ samples $\boldsymbol{\theta}_{j,i}^{(s)} \sim p(\boldsymbol{\theta})$ but restricted only to those in $\Theta^{(s)}$ (see below for one approach to this selective sampling), and compute their corresponding likelihoods $\mathcal{L}(\boldsymbol{\theta}_{j,i}^{(s)})$. Then, the fraction of probability mass in stratum s that exceeds likelihood λ_i is estimated with

$$\hat{\chi}_i^{(s)} = \frac{1}{N_{i,\text{cum}}^{(s)}} \sum_{j=1}^{N_i^{(s)}} \mathbb{I}_{\tilde{\Theta}_i}(\boldsymbol{\theta}_{j,i}^{(s)}) \quad (21)$$

where $N_{i,\text{cum}}^{(s)} = \sum_{l=1}^i N_l^{(s)}$ is the cumulative number of stratum s samples up through iteration i , i.e., all of the previous samples from stratum s are retained and re-used. If $p^{(s)} = \mathbb{P}(\boldsymbol{\theta} \in \Theta^{(s)})$ is the total probability mass in stratum s , then the combined estimate of the probability mass with likelihood exceeding λ_i is

$$\hat{\chi}_i^{\text{SS}} = \sum_{s \in \mathcal{I}_{i-1}} p^{(s)} \hat{\chi}_i^{(s)} \quad (22)$$

The mean of this estimate is $\mathbb{E}[\hat{\chi}_i^{\text{SS}}] = \chi_i$ and its variance is

$$\text{Var}[\hat{\chi}_i^{\text{SS}}] = \frac{\sigma_{\chi_i}^2}{N_{i,\text{cum}}} - \frac{1}{N_{i,\text{cum}}} \sum_{s \in \mathcal{I}_{i-1}} \left(\hat{\chi}_i^{(s)} - \hat{\chi}_i^{\text{SS}} \right)^2 p^{(s)} \quad (23)$$

where $N_{i,\text{cum}} = \sum_{s=1}^{\bar{n}_{\text{st}}} N_{i,\text{cum}}^{(s)}$ and $\sigma_{\chi_i}^2$ is the variance of $\chi(\lambda_i)$.

Finally, the marginal likelihood (3) is estimated, using a rectangle-rule integration, with

$$\hat{\mathcal{E}}^{\text{SS}} = \sum_i \lambda_i (\hat{\chi}_{i-1}^{\text{SS}} - \hat{\chi}_i^{\text{SS}}) \quad (24)$$

Algorithm 2 shows the steps for this stratified sampling likelihood-level adapted estimation of the marginal likelihood \mathcal{E} , where the initial strata index set \mathcal{I}_0 includes all strata but, as the iterations progress, samples are obtained from a smaller number of strata that contain

Algorithm 2: Likelihood level adapted marginal likelihood estimation using stratified sampling (LLA-SS).

- 1 **Initialization:** Set $\widehat{\chi}_0^{\text{SS}} = 1$, $\widehat{\mathcal{E}}_0^{\text{SS}} = 0$, and $\lambda_0 = 0$
 - 2 Divide the sample space into \bar{n}_{st} strata $\{\Theta^{(s)}\}_{s=1}^{\bar{n}_{\text{st}}}$
 - 3 Set the initial strata index set $\mathcal{I}_0 = \{1, \dots, \bar{n}_{\text{st}}\}$ to contain all strata.
 - 4 Set $i = 1$
 - 5 **while** *Stopping Criterion* = *FALSE* **do**
 - 6 **for** $s \in \mathcal{I}_{i-1}$ **do**
 - 7 Set $N_i^{(s)} = N/|\mathcal{I}_{i-1}|$, where $|\cdot|$ here denotes the number of strata in the set
 - 8 Draw $N_i^{(s)}$ additional samples $\theta_{j,i}^{(s)} \sim p(\theta)$ from stratum $\Theta^{(s)}$ for
 $j = 1, \dots, N_i^{(s)}$
 - 9 Calculate likelihood values $\mathcal{L}(\theta_{j,i}^{(s)})$ for these samples
 - 10 Assign weights $w_i^{(s)} = p^{(s)}/N_{i,\text{cum}}^{(s)}$ where $p^{(s)} = \mathbb{P}(\theta \in \Theta^{(s)})$ and
 $N_{i,\text{cum}}^{(s)} = \sum_{l=1}^i N_l^{(s)}$
 - 11 Select a suitable new likelihood level $\lambda_i > \lambda_{i-1}$ (see Section 4.4)
 - 12 Estimate $\widehat{\chi}_i^{\text{SS}} = \sum_{s \in \mathcal{I}_{i-1}} w_i^{(s)} \sum_{j=1}^{N_i^{(s)}} \mathbb{I}_{\tilde{\Theta}_i}(\theta_{j,i}^{(s)})$
 - 13 Update the marginal likelihood $\widehat{\mathcal{E}}_i^{\text{SS}} = \widehat{\mathcal{E}}_{i-1}^{\text{SS}} + \lambda_i (\widehat{\chi}_{i-1}^{\text{SS}} - \widehat{\chi}_i^{\text{SS}})$
 - 14 Let $\mathcal{I}_i = \{s \mid \max_j \mathcal{L}(\theta_{j,i}^{(s)}) > \lambda_i\}$, which will be used in the next iteration, be
the set of all strata with at least one sample $\theta_{j^*,i}^{(s)}$ having likelihood greater than
 λ_i
 - 15 $i \leftarrow i + 1$
- Result:** The marginal likelihood $\widehat{\mathcal{E}}_{\text{final}}^{\text{SS}}$
-

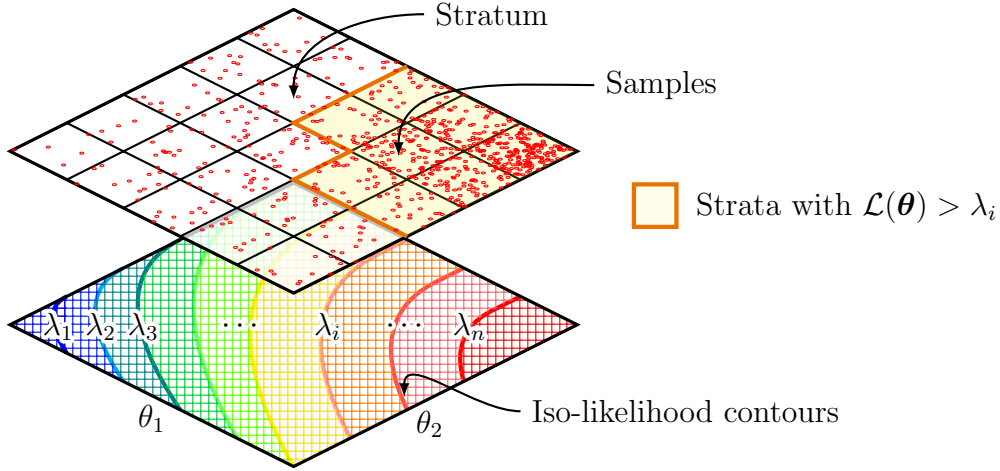


Figure 3: Likelihood level adapted stratified sampling (LLA-SS) method: the iso-likelihood contours are shown with $\lambda_1 < \lambda_2 < \dots < \lambda_n$; more samples are generated from the strata with high likelihood values. For example, the shaded strata with the thick boundary lines have at least one sample with $\mathcal{L}(\boldsymbol{\theta}) > \lambda_i$.

likelihood values larger than prior likelihood levels. Figure 3 depicts a schematic of the LLA-SS algorithm for a two-dimensional parameter vector $\boldsymbol{\theta}$, showing a shaded region that contains the strata with $\mathcal{L}(\boldsymbol{\theta}) > \lambda_i$ from which additional samples are drawn.

One way to construct the strata to sample $\boldsymbol{\theta} = [\theta_1, \theta_2, \dots, \theta_{n_\theta}]^T$ from the joint probability density $p(\boldsymbol{\theta}) = \prod_{k=1}^{n_\theta} p(\theta_k)$ — *i.e.*, if the elements of $\boldsymbol{\theta}$ are independent — is to use the inverses of the marginal cumulative density functions $F_{\theta_k}(\cdot)$. For stratum s , let

$$\boldsymbol{\Theta}^{(s)} = \Theta_1^{(s)} \times \Theta_2^{(s)} \times \dots \times \Theta_{n_\theta}^{(s)} \quad (25)$$

where $\Theta_k^{(s)} = \left\{ F_{\theta_k}^{-1}(y) \mid y \in \left(\frac{s-1}{n_{\text{st}}}, \frac{s}{n_{\text{st}}} \right] \right\}$ so that $\mathbb{P}(\boldsymbol{\theta} \in \boldsymbol{\Theta}^{(s)}) = \prod_{i=1}^{n_\theta} (1/n_{\text{st}}) = 1/\bar{n}_{\text{st}}$. Implementing stratified sampling can be difficult with high-dimensional parameter spaces (*i.e.*, large n_θ). However, as this LLA-SS iterates, only a very few strata will remain with $\mathcal{L}(\boldsymbol{\theta}) > \lambda_i$ because the high-likelihood regions are often concentrated in a small portion of the parameter space.

3.4. Likelihood level adapted Markov chain Monte Carlo (LLA-MCMC)

In the following proposed algorithm, the Markov chain Monte Carlo method [54] is used in a sequential manner. As the likelihood level λ_i increases with iteration, $\tilde{\boldsymbol{\Theta}}_i \subset \tilde{\boldsymbol{\Theta}}_{i-1}$, where

$\tilde{\Theta}_i$ is defined in (18). Hence, at iteration i , χ_i can be written as [58, 59]

$$\begin{aligned}
\chi_i &= \mathbb{P}(\boldsymbol{\theta} \in \tilde{\Theta}_i) = \prod_{k=1}^i \mathbb{P}(\boldsymbol{\theta} \in \tilde{\Theta}_k | \boldsymbol{\theta} \in \tilde{\Theta}_{k-1}) \\
&= \mathbb{P}(\boldsymbol{\theta} \in \tilde{\Theta}_i | \boldsymbol{\theta} \in \tilde{\Theta}_{i-1}) \prod_{k=1}^{i-1} \mathbb{P}(\boldsymbol{\theta} \in \tilde{\Theta}_k | \boldsymbol{\theta} \in \tilde{\Theta}_{k-1}) \\
&= \frac{\mathbb{P}(\boldsymbol{\theta} \in \tilde{\Theta}_i)}{\mathbb{P}(\boldsymbol{\theta} \in \tilde{\Theta}_{i-1})} \hat{\chi}_{i-1} \\
&\approx \hat{\chi}_{i-1} \frac{\sum_{j=1}^N [\mathbb{I}_{\tilde{\Theta}_i}(\boldsymbol{\theta}_{j,i})]}{\sum_{j=1}^N [\mathbb{I}_{\tilde{\Theta}_{i-1}}(\boldsymbol{\theta}_{j,i-1})]}
\end{aligned} \tag{26}$$

where $\tilde{\Theta}_0 \equiv \Theta$ and $\{\boldsymbol{\theta}_{j,l}\}_{l>0}$, $j = 1, \dots, N$, are obtained from Markov chains with $\boldsymbol{\theta}_{j,0} \sim p(\boldsymbol{\theta})$ with a transition kernel that can be assumed of the form $K(\boldsymbol{\theta}, d\eta)$ given in (13). Hence, starting with $\hat{\chi}_0 = 1$, $\hat{\chi}_i$ can be estimated in the i th iteration by sampling from Markov chains that are initiated with the previous iteration's samples $\{\boldsymbol{\theta}_{j,i-1}\}_{j=1}^N$, each satisfying $\mathcal{L}(\boldsymbol{\theta}_{j,i-1}) > \lambda_{i-1}$. Note that, for a high-dimensional parameter space, a Markov chain with a higher acceptance rate is used herein, *e.g.*, the modified Metropolis-Hastings algorithm (MMH) [56]. An algorithm for likelihood-level adapted estimation of marginal likelihood or evidence using a Markov chain is presented in Algorithm 3, where $p_i(\boldsymbol{\theta}) = p(\boldsymbol{\theta} | \boldsymbol{\theta} \in \tilde{\Theta}_i)$ are successively defined and samples are drawn from them using the Markov chain Monte Carlo method. A schematic of this algorithm, with the Markov chain propagating samples to higher likelihood regions, is shown in Figure 4. In the figure, Markov chains are shown to propagate to high-likelihood regions as samples are drawn from them.

4. Discussion of the Proposed Approach

4.1. Estimation of posterior moments

The posterior statistics of the model parameters are often sought from a Bayesian analysis. Using the proposed approach herein, the samples corresponding to each of the likelihood levels from the three algorithms can also be used to evaluate the posterior moments of the model parameters $\boldsymbol{\theta}$, using the rejected samples and the change in evidence value at each step, without any significant computation cost. For example, the mean and variance of $\boldsymbol{\theta}$ can be evaluated using

$$\begin{aligned}
\mathbb{E}[\boldsymbol{\theta}] &\approx \frac{1}{\hat{\mathcal{E}}_{\text{final}}} \sum_{i=1}^{i_{\text{final}}} \Delta \hat{\mathcal{E}}_i \bar{\boldsymbol{\theta}}_i \\
\text{Var}[\boldsymbol{\theta}] &\approx \frac{1}{\hat{\mathcal{E}}_{\text{final}}} \sum_{i=1}^{i_{\text{final}}} \Delta \hat{\mathcal{E}}_i \bar{\boldsymbol{\theta}}_i^2 - (\mathbb{E}[\boldsymbol{\theta}])^2
\end{aligned} \tag{27}$$

Algorithm 3: Likelihood level adapted marginal likelihood estimation using particle approximation (LLA-MCMC).

- 1 **Initialization:** Set $\hat{\chi}_0^{\text{MCMC}} = 1$, $\hat{\mathcal{E}}_0^{\text{MCMC}} = 0$, $\lambda_0 = 0$, and $p_0(\boldsymbol{\theta}) = p(\boldsymbol{\theta})$
- 2 Draw N samples $\{\boldsymbol{\theta}_{j,0}\}_{j=1}^N$ from the distribution $p_0(\boldsymbol{\theta})$
- 3 Set $i = 1$
- 4 **while** *Stopping Criterion* = *FALSE* **do**
- 5 Select a suitable new likelihood level $\lambda_i > \lambda_{i-1}$ (see Section 4.4)
- 6 Define $p_i(\boldsymbol{\theta}) = p(\boldsymbol{\theta} | \boldsymbol{\theta} \in \tilde{\Theta}_i)$
- 7 Identify the samples $\{\boldsymbol{\theta}_{j,i}\}_{j=1}^{N_{\text{pass}}}$ satisfying $\mathcal{L}(\boldsymbol{\theta}_{j,i}) > \lambda_i$
- 8 Remove the rest of the samples with $\mathcal{L}(\boldsymbol{\theta}_{j,i}) \leq \lambda_i$
- 9 Draw samples from the distribution $p_i(\boldsymbol{\theta})$ by running Markov chains starting from $\{\boldsymbol{\theta}_{j,i}\}_{j=1}^{N_{\text{pass}}}$ to replace samples with $\mathcal{L}(\boldsymbol{\theta}_{j,i}) \leq \lambda_i$
- 10 Evaluate likelihood values $\mathcal{L}(\boldsymbol{\theta}_{j,i})$ for the newly drawn samples
- 11 Estimate $\hat{\chi}_i^{\text{MCMC}} = \hat{\chi}_{i-1}^{\text{MCMC}} \sum_{j=1}^N \mathbb{I}_{\tilde{\Theta}_i}(\boldsymbol{\theta}_{j,i-1})/N$
- 12 Update the marginal likelihood $\hat{\mathcal{E}}_i^{\text{MCMC}} = \hat{\mathcal{E}}_{i-1}^{\text{MCMC}} + \lambda_i (\hat{\chi}_{i-1}^{\text{MCMC}} - \hat{\chi}_i^{\text{MCMC}})$
- 13 $i \leftarrow i + 1$

Result: The marginal likelihood $\hat{\mathcal{E}}_{\text{final}}^{\text{MCMC}}$

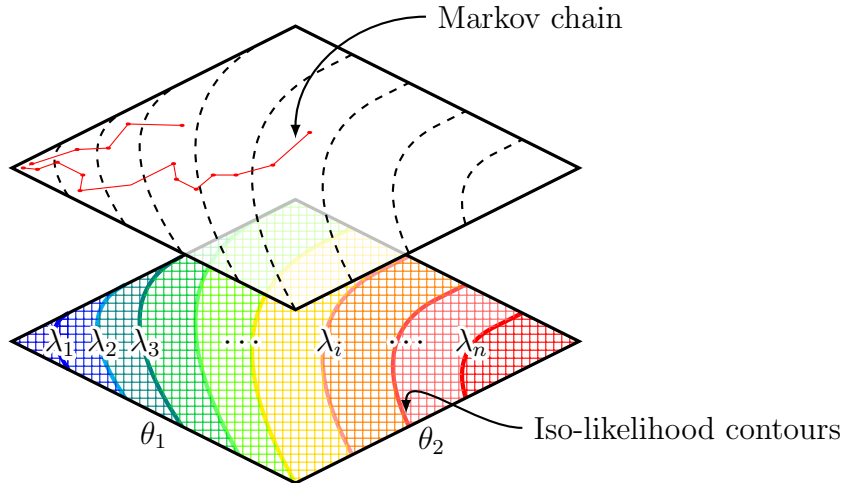


Figure 4: Likelihood level adapted particle approximation (LLA-MCMC) method: the iso-likelihood contours are shown with $\lambda_1 < \lambda_2 < \dots < \lambda_n$; Markov chains are run to generate samples with $\mathcal{L}(\boldsymbol{\theta}) > \lambda_i$ starting from a sample with $\mathcal{L}(\boldsymbol{\theta}) > \lambda_{i-1}$.

where $\Delta\widehat{\mathcal{E}}_i = \lambda_i(\widehat{\chi}_{i-1} - \widehat{\chi}_i)$ and $\bar{\boldsymbol{\theta}}_i$ is either the mean or a randomly chosen sample (which avoids the estimation of the mean of parameters at every level) from $\{\boldsymbol{\theta}_{j,i} | \mathcal{L}(\boldsymbol{\theta}_i) \in [\lambda_{i-1}, \lambda_i]\}$ that has been used to estimate χ_i .

4.2. Stopping criteria

Different stopping criteria, based on accuracy and/or computational cost, can be used in these algorithms, namely: (i) the change in evidence is less than some threshold $\Delta\mathcal{E}_{\text{tol}}$, often taken to be 1% or 0.1%; (ii) the total number of iterations exceeds a pre-chosen number i_{final} ; (iii) $\widehat{\chi}_i$ is less than some pre-specified tolerance χ_{tol} ; and/or (iv) the number of sample likelihood calculations has exceeded some threshold. The examples herein utilize one or more of these stopping criteria. While not used herein, an additional criterion could be to stop when the likelihood level λ_i of the current iteration is within some fraction of the theoretical maximum of the likelihood function (if known).

4.3. Accuracy

If $\chi_{\text{final}} \equiv \chi_{i_{\text{final}}}$ is the final (*i.e.*, after iteration i_{final}) probability mass contained in regions with likelihoods greater than $\lambda_{\text{final}} \equiv \lambda_{i_{\text{final}}}$, the evidence in (16) can be written as [60]

$$\begin{aligned}
\mathcal{E} &= \int_0^1 \varphi(\chi) d\chi \\
&= \sum_{i=1}^{i_{\text{final}}} \lambda_i \Delta\widehat{\chi}_i + \underbrace{\int_0^{\chi_{\text{final}}} \varphi(\chi) d\chi}_{\epsilon_t} + \underbrace{\left[\int_{\chi_{\text{final}}}^1 \varphi(\chi) d\chi - \sum_{i=1}^{i_{\text{final}}} \lambda_i \Delta\chi(\lambda_i) \right]}_{\epsilon_n} \\
&\quad + \underbrace{\sum_{i=1}^{i_{\text{final}}} \lambda_i [\Delta\chi(\lambda_i) - \Delta\widehat{\chi}_i]}_{\epsilon_s} \\
&= \sum_{i=1}^{i_{\text{final}}} \lambda_i \Delta\widehat{\chi}_i + \epsilon_t + \epsilon_n + \epsilon_s
\end{aligned} \tag{28}$$

where $\Delta\widehat{\chi}_i = (\widehat{\chi}_{i-1} - \widehat{\chi}_i)$ is an estimate of $\Delta\chi(\lambda_i) = \chi(\lambda_{i-1}) - \chi(\lambda_i)$, ϵ_t is the truncation error, ϵ_n is the numerical integration error, and ϵ_s is the stochastic error.

Since the algorithms are halted when $\chi = \chi_{\text{final}} \ll 1$, rather than at $\chi = 0$, the truncation error ϵ_t arises; however, ϵ_t is very small if a sufficient number of iterations are used. If $d\varphi/d\chi$ is bounded in $[\chi_{\text{final}}, 1]$, the numerical integration error ϵ_n in the proposed algorithms for a rectangular rule is of the order $\mathcal{O}(N^{-1})$, where N is the number of samples. Finally, the stochastic error ϵ_s is asymptotically unbiased with a convergence rate of $\mathcal{O}(N^{-1/2})$ for the methods used here, as shown in Appendix A. Hence, the convergence of ϵ_s dictates the convergence of the algorithms here due to its slower dependence on $N^{-1/2}$.

4.4. Choice of likelihood levels

The numerical integration error ϵ_n can be reduced by using very small increments in χ , which, however, leads to higher computational cost. On the other hand, choosing $\chi_{i-1} \gg \chi_i$ will lead to an inaccurate estimate of the marginal likelihood. Note that the increment in χ_i depends on the selection of λ_i . Hence, to ensure that the increments in χ are not very large, small increments in λ are suggested. For example, based on the computational budget and required accuracy, λ_i can be assumed of the form $\lambda_i = 10^\alpha \lambda_{i-1}$ with $\alpha > 0$ chosen accordingly. Another strategy, utilized in the numerical examples herein, is to choose λ_i as the N_i^{reject} th lowest likelihood value, where $N_i^{\text{reject}} = \lceil f_i^{\text{reject}} N_i \rceil$ for some fixed $f_i^{\text{reject}} \in (0, 1)$. Note that, at the first few iterations, a fixed but large f^{reject} may result in $\lambda_i < \lambda_{i-1}$. To avoid this f^{reject} is ramped up gradually during the initial iterations to a fixed maximum value in this paper. Nonetheless, if $\lambda_i < \lambda_{i-1}$ is observed, f^{reject} is increased to avoid any such issues.

5. Numerical Illustrations

The three proposed methods for evaluating the evidence are compared against other established approaches through a series of four examples in this section. While the first example has an exact solution for the marginal likelihood, a standard Monte Carlo-based sampling approach is treated as the ground truth evidence value in the final three examples. Examples I and II present comparisons against MultiNest, whereas Examples II, III, and IV provide comparisons against nested sampling. A high-level comparison of some of the characteristics of the algorithms implemented within this study is given in Table 1. These features include the capability for implementation in parallel computation (parallelizability), how well the method scales to high-dimensional problems (scalability), the ability to handle multi-modal likelihood functions (multi-modal), and the number of hyper-parameters that must be tuned (implementation complexity).

Table 1 shows that the standard Monte Carlo approach is (embarrassingly) parallelizable and only has one hyper-parameter, *i.e.*, the number of samples, but it is significantly inefficient in higher dimensions and for multi-modal distributions. As mentioned previously, traditional nested sampling struggles with efficiency, whereas MultiNest is well-suited to handle multi-modal distributions. Traditional nested sampling is more efficient for high-dimensional spaces compared to MultiNest as noted in Example IV, though recent developments in MultiNest have enabled a certain degree of parallelization [44]. Both nested sampling and MultiNest require specifying the number of active points and the stopping criterion, which is based on either the total number of iterations or achieving some tolerance related to the change in evidence. In addition, MultiNest has an additional hyper-parameter for the target efficiency. In this paper, the hyperparameters for MultiNest are chosen to be consistent with those used for Nested Sampling, whereas the hyperparameters for the three proposed algorithms are chosen to provide comparable results.

Among the three proposed methodologies, LLA-IS lacks the capability for parallelization and is not well-suited to explore high-dimensional space. LLA-IS also features three hyper-parameters, including the number of initial samples and the standard deviation of

Table 1: Comparison of the computational capabilities of the algorithms implemented in this study

Algorithm	Parallelizability	Scalability	Multi-Modal	Hyperparameters
Monte Carlo	Perfectly	Inefficiently	Yes	1. # of samples
Nested Sampling	No	Inefficiently	No	1. # of active points 2. Stopping criterion
MultiNest	Yes	No	Well-suited	1. # of active points 2. Target efficiency 3. Stopping criterion
LLA-IS	No	No	Depends on ISD choice	1. # of initial samples 2. Gaussian ISD std. 3. Fraction of likelihood level
LLA-SS	Yes	No	Yes	1. # of strata 2. Fraction of likelihood level
LLA-MCMC	Yes	Efficiently	With modifications	1. # of initial samples 2. # of samples being replaced 3. Gaussian proposal density std. 4. Stopping criterion

the importance density, both of which can be tuned with respect to the available computational power and model complexity. Both the LLA-IS and LLA-SS methods feature a hyper-parameter related to the “fraction of likelihood level,” which must be tuned as described in Section 4.4. The advantage of LLA-SS is its fast implementation (thanks to parallelization) and high accuracy for low-dimensional space. The hyper-parameter for the number of substrata for each parameter can also be fixed (herein 5 is used). The proposed LLA-MCMC approach can also be applied in parallel; its strength, however, is in its scalability, as is powerfully demonstrated in Example IV. Its stopping criterion hyper-parameter can be determined based on Section 4.2. The other three hyper-parameters are selected based on model complexity and available computational power. Like standard Monte Carlo sampling, the LLA-SS algorithm can handle multi-modal likelihood functions, but it is not as well-suited as MultiNest. The LLA-IS and LLA-MCMC algorithms can also be used for such likelihood functions, but LLA-IS requires a carefully chosen importance density function $q(\theta)$, and LLA-MCMC requires further modifications [61] (that replace the MH algorithm used herein with different MCMC algorithms).

5.1. Example I: Conceptual example

Consider a simple multivariate Gaussian likelihood function for a dataset $\mathfrak{D} = \{x_i\}_{i=1}^n$ defined by

$$\mathcal{L}(\mu) = p(\mathfrak{D} | \mu) = \frac{1}{(2\pi)^{n/2}\sigma^n} \exp\left(-\frac{1}{2\sigma^2} \sum_{i=1}^n (x_i - \mu)^2\right) \quad (29)$$

The prior for the parameter μ is assumed to be a normal distribution with mean and variance given by μ_0 and σ_0^2 , respectively, *i.e.*,

$$p(\mu | \mu_0, \sigma_0^2) = \frac{1}{\sqrt{2\pi\sigma_0^2}} \exp\left(-\frac{(\mu - \mu_0)^2}{2\sigma_0^2}\right) \quad (30)$$

On the other hand, the standard deviation σ of the likelihood function is assumed constant and known. The evidence or marginal likelihood in this example can be easily computed [62]

$$\mathcal{E}_{\text{exact}} = \frac{\sigma}{\left(\sqrt{2\pi\sigma^2}\right)^n \sqrt{n\sigma_0^2 + \sigma^2}} \exp\left(-\frac{\sum_{i=1}^n x_i^2}{2\sigma^2} - \frac{\mu_0^2}{2\sigma_0^2}\right) \times \exp\left(\frac{2n\mu_0\bar{x} + \frac{\sigma_0^2 n^2 \bar{x}^2}{\sigma^2} + \frac{\sigma^2 \mu_0^2}{\sigma_0^2}}{2(n\sigma_0^2 + \sigma^2)}\right) \quad (31)$$

With $n = 100$ measurements generated from a normal distribution with mean 1.5 and standard deviation 0.5, the three proposed algorithms are implemented using $\mu_0 = 1$ and $\sigma_0 = 0.25$. The stopping criteria, as discussed in section 4.2, use evidence change threshold $\Delta\mathcal{E}_{\text{tol}} = 0.01\%$, lower bound tolerance $\chi_{\text{tol}} = 0.005$, maximum iteration count $i_{\text{max}} = 100$, and the number of likelihood evaluations is limited to 20,000. The algorithms are stopped as soon as any of these criteria is met.

The MultiNest nested sampling algorithm is implemented using $N_{\text{live}} = 1000$ active points. LLA-IS is implemented with a Gaussian importance density formed at each iteration using the mean of the retained samples and a smaller standard deviation of 0.125 (*i.e.*, a smaller spread) with an initial sample size of $N = 1000$. The likelihood levels are decided at every iteration based on the fraction $f_i^{\text{reject}} = \min(0.3, 0.025i)$. The LLA-SS algorithm is used with $\Theta^{(s)} = \left\{F_{\mu}^{-1}(y) \mid y \in \left(\frac{s-1}{n_{\text{st}}}, \frac{s}{n_{\text{st}}}\right]\right\}$, where $n_{\text{st}} = 5$, and F_{μ} is the cumulative probability distribution of the parameter μ . For this algorithm, the likelihood levels are decided at every iteration based on the fraction $f_i^{\text{reject}} = \min(0.9, 0.025i)$. The LLA-MCMC algorithm is implemented with an initial sample size of $N = 1000$ and, at each iteration, the 25 samples with the lowest likelihoods are rejected and 25 new samples with higher likelihoods are added to the sample pool.

Table 2 shows a comparison of the marginal likelihoods or evidence values obtained using the three proposed algorithms, MultiNest, and the exact value computed using (31). Note that the (natural) log of the evidence is used in reporting the results herein as the evidence can be orders of magnitude larger or smaller depending on the problem. Coefficient of variation (COV) is also used in this example to facilitate comparisons across multiple runs. The table shows that all three proposed algorithms provide log evidences that are accurate within 0.4% and exhibit very small coefficients of variation. Notably, the proposed LLA-SS outperforms MultiNest in terms of both accuracy and consistency via its lower error and COV, respectively. Figure 5 shows how these algorithms reduce error with increasing computational effort. The figure also indicates that the LLA-SS algorithm outperforms the others (thought it will suffer from the curse of dimensionality as the parameter space dimension increases). The figure also shows that the COV of LLA-MCMC is much larger than those of the other algorithms because the samples from Markov chain Monte Carlo methods are generally correlated; this increased variation can be ameliorated by selecting every n^{th} sample from the chain, where $n \gg 1$.

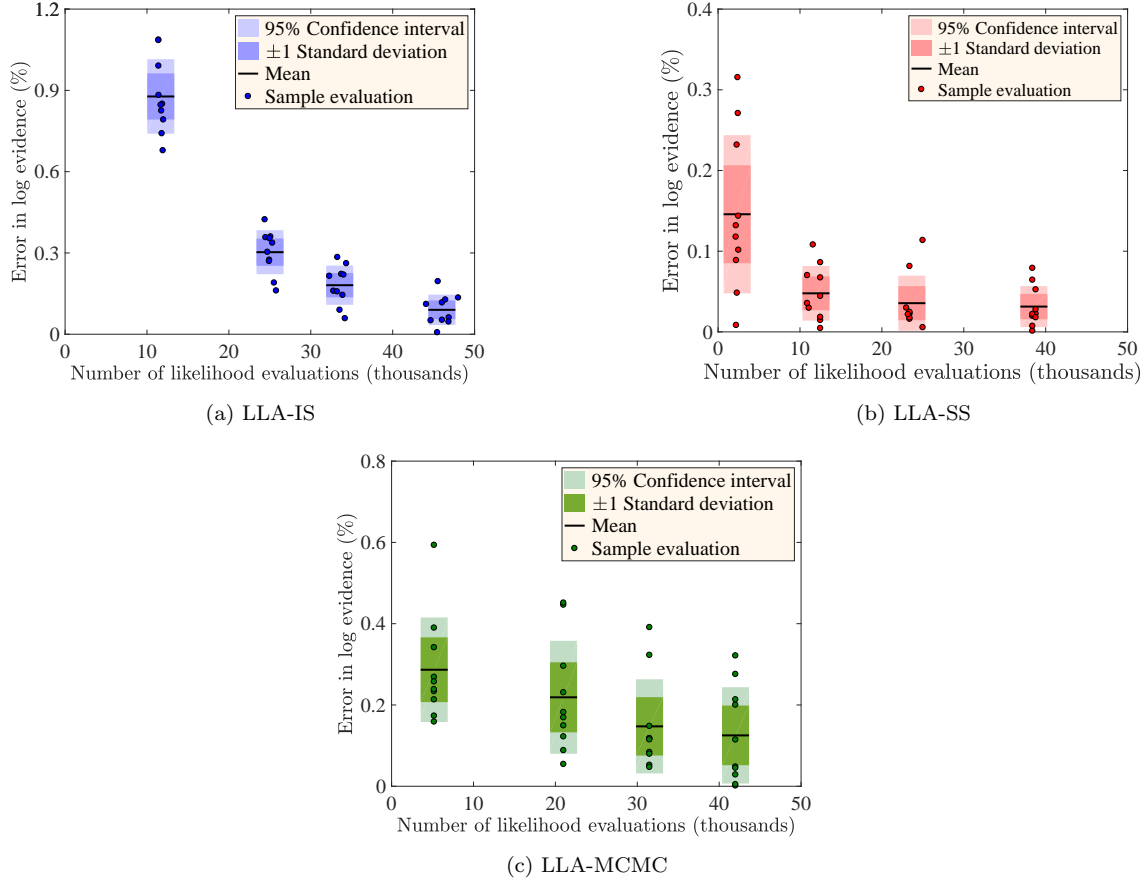


Figure 5: The error in the estimation of log evidence is reduced with increasing number of likelihood function evaluations for the three proposed algorithms. Note that the three vertical scales are not the same.

Table 2: Comparison of the first example’s marginal likelihoods obtained using the three proposed algorithm along with the exact value. The errors and coefficients of variations (COV) of the log evidence are obtained from 10 independent simulation runs.

Method	# fcn. evals [†]	$\log_e(\text{Evidence})$	Error (%)	COV (%)
Exact	—	−69.8354	—	—
MultiNest ($N_{\text{live}} = 1000$)	~ 8,000	−69.8565	0.0302	0.0512
LLA-IS	~ 12,000	−70.0468	0.3028	0.0812
LLA-SS	~ 10,000	−69.8274	0.0113	0.0415
LLA-MCMC	~ 10,500	−69.7469	0.1267	0.1188

[†] Since the number of function evaluations slightly varies for multiple runs, an approximate number is provided.

5.2. Example II: 11 story base isolated building

This example utilizes a superstructure comprised of an 11-story 2-bay 99 DOF superstructure [63], sitting on a hysteretic isolation layer that is rigid in-plane and can only move

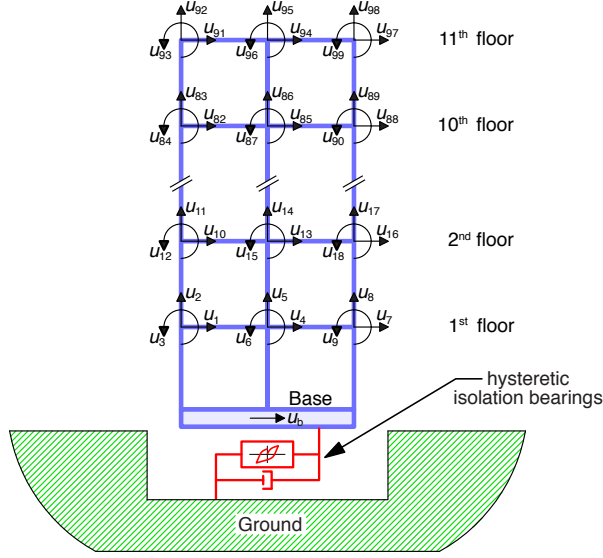


Figure 6: 100 DOF base-isolated structural model

horizontally, resulting in the 100 DOF model shown in Figure 6. Rayleigh damping, with assumed 3% damping ratios for the 1st and 10th mode, is used to construct the superstructure damping matrix. If considered as a fixed base structure, the superstructure would have a fundamental period of 1.05 s with equations of motion written as

$$\mathbf{M}_s \ddot{\mathbf{u}}_s + \mathbf{C}_s \dot{\mathbf{u}}_s + \mathbf{K}_s \mathbf{u}_s = -\mathbf{M}_s \mathbf{r}_s \ddot{u}_g \quad (32)$$

where \mathbf{M}_s , \mathbf{C}_s and \mathbf{K}_s are the mass, damping and stiffness matrices of the superstructure, respectively; \ddot{u}_g is the ground acceleration; \mathbf{u}_s is the generalized displacement vector relative to the ground, consisting of 3 DOF per node for each of the 33 nodes in the superstructure. The influence vector of the ground motion \ddot{u}_g , consisting of a 1 in each element corresponding to a horizontal displacement in \mathbf{u}_s and zeros elsewhere, is denoted by \mathbf{r}_s . When combined with the isolation layer, the equations of motion are

$$\mathbf{M}_s \ddot{\mathbf{u}}_s + \mathbf{C}_s \dot{\mathbf{u}}_s + \mathbf{K}_s \mathbf{u}_s = -\mathbf{M}_s \mathbf{r}_s \ddot{u}_g + \mathbf{C}_s \mathbf{r}_s \dot{u}_b + \mathbf{K}_s \mathbf{r}_s u_b \quad (33)$$

$$m_b \ddot{u}_b + (c_b + \mathbf{r}_s^T \mathbf{C}_s \mathbf{r}_s) \dot{u}_b + \mathbf{r}_s^T \mathbf{K}_s \mathbf{r}_s u_b + f_b = -m_b \ddot{u}_g + \mathbf{r}_s^T \mathbf{C}_s \dot{\mathbf{u}}_s + \mathbf{r}_s^T \mathbf{K}_s \mathbf{u}_s \quad (34)$$

where u_b is the isolation layer drift; m_b is the mass of the base; c_b is the isolation layer linear damping coefficient; f_b is the isolation layer restoring force, which can be modeled in a number of ways, including a Bouc-Wen model [64], a bilinear model and various “equivalent” linear models (see Figure 8). The “true” model here, used to generate the data \mathfrak{D} , is a Bouc-Wen model with

$$\begin{aligned} f_b &= k_{\text{post}} u_b + (1 - r_k) Q_y z \\ \dot{z} &= A \dot{u}_b - \beta \dot{u}_b |z|^{n_{\text{pow}}} - \gamma z |\dot{u}_b| |z|^{n_{\text{pow}}-1} \end{aligned} \quad (35)$$

where k_{pre} and k_{post} are the isolator pre-yield and post-yield stiffnesses, respectively; Q_y is the isolator yield force; $(1 - r_k)Q_y$, the peak of the non-elastic force, depends on the hardening ratio $r_k = k_{\text{post}}/k_{\text{pre}}$; z is an evolutionary variable; and the Bouc-Wen hysteresis shaping constants are chosen $A = 2\beta = 2\gamma = k_{\text{pre}}/Q_y$ so that z remains in $[-1, 1]$ and produces in f_b identical loading and unloading stiffnesses.

Table 3: Exact and prior distribution of parameters for the 11-story base isolated building.

Parameter	True value	Prior Distribution	Lower bound	Upper bound	Mean	Std. dev.
k_{post} (kN/m)	750	Trunc. Gaussian	700	800	780	20
Q_y ($\%W^\ddagger$)	5	Uniform	4.5	6.5	5.5	0.5774
r_k	0.1667	Uniform	0.16	0.20	0.18	0.0115

$^\ddagger W$ = total weight of the building.

To generate the measurement data, the isolation-layer linear damping coefficient is assumed as $c_b = 40$ kN·s/m. Further, $k_{\text{post}} = 750$ kN/m, yield force $Q_y = 5\%$ of building weight and hardening ratio $r_k = k_{\text{post}}/k_{\text{pre}} = 1/6$ are used [65]. These parameters give the first mode a typical large-displacement isolation period of $T_1^i = 2.76$ s, and a linear viscous damping ratio of 5.5% (not including any energy dissipation from the isolator hysteresis). The ground excitation is the 1940 El Centro earthquake record (peak ground acceleration 3.43 m/s) of 30 s duration with a sampling rate of 20 Hz recorded at Imperial Valley Irrigation District substation in El Centro, California. The absolute (horizontal) acceleration of the roof, specified by DOF u_{97} in Figure 6, with a sampling rate of 20 Hz is used as the model output, to which is added a zero-mean Gaussian measurement-noise pulse process with a standard deviation that is 20% of the standard deviation of the exact response.

The uncertain parameters are the post-yield stiffness, the isolator yield force and the hardening ratio r_k . The assumed priors for these uncertain parameters $\boldsymbol{\theta} = \{k_{\text{post}}, Q_y, r_k\}^T$ are given in Table 3. The MultiNest algorithm is applied using 1000 active points. The LLA-IS algorithm is implemented with a Gaussian importance density formed at each iteration using the mean of the current samples and standard deviations and with $\gamma_S = 0.5N$ and an initial sample size of $N = 100$. The likelihood levels are decided at every iteration based on the fraction $f_i^{\text{reject}} = \min(0.5, 0.1 + 0.025(i - 1))$. The LLA-SS algorithm is implemented with $\Theta_k^{(s)} = \left\{ F_{\theta_k}^{-1}(\theta_k) \mid \theta_k \in \left(\frac{s-1}{n_{\text{st}}}, \frac{s}{n_{\text{st}}} \right] \right\}$, where $n_{\text{st}} = 5$, and $F_{\theta_k}^{-1}$ is the inverse probability distribution of θ_k , $k = 1, \dots, 3$. For this algorithm, the likelihood levels are decided at every iteration based on the fraction $f_i^{\text{reject}} = 0.25$. The LLA-MCMC algorithm is implemented with an initial sample size of 100 and, at each iteration, the 10 samples with the lowest likelihoods are rejected and 10 new samples with higher likelihoods are added to the sample pool using the Metropolis-Hastings algorithm. The proposal density in the Metropolis-Hastings algorithm is assumed Gaussian with standard deviations of 5 kN/m, 0.5%, and 0.005 for the parameters k_{post} , Q_y , and r_k , respectively. The stopping criteria are used as in Example I except that the total number of function evaluation is limited to 7000 and

$\Delta\mathcal{E}_{\text{tol}} = 1\%$ to limit computational cost.

Since the analytical value of the marginal likelihood is not available for this example, the accuracies of the proposed algorithms are compared in Table 4 with the Monte Carlo and nested sampling [42] algorithms. The relative difference in the marginal likelihood or evidence is calculated using

$$\text{Relative difference} = \left| \frac{\log \hat{\mathcal{E}}^{\text{LLA}} - \log \hat{\mathcal{E}}^{\text{MC}}}{\log \hat{\mathcal{E}}^{\text{MC}}} \right| \quad (36)$$

where $\hat{\mathcal{E}}^{\text{MC}}$ is estimated with Monte Carlo sampling using many likelihood evaluations. Figure 7 is used to determine the sufficient number of likelihood evaluations needed to produce a stable estimate, which is then compared to evidence estimates from other methods. Among

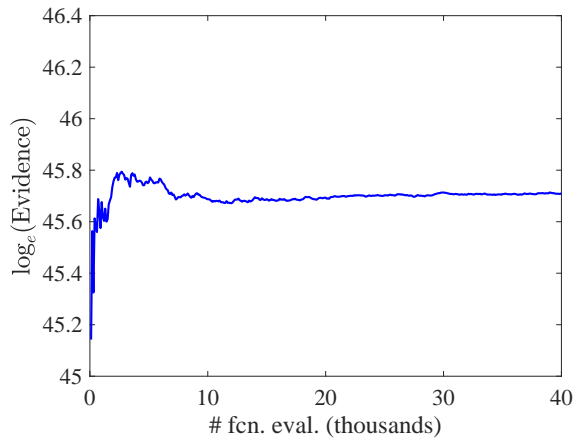


Figure 7: Estimation of evidence using Monte Carlo approach with increasing number of likelihood evaluations.

the three algorithms, the performance of LLA-IS is affected by the assumption of importance density at each iteration since the importance density is not efficient in drawing samples from the high-likelihood region. and performs poorly compared to all other algorithms. This shows that Gaussian importance densities might not be appropriate for all the problems and a judicious choice of $q(\boldsymbol{\theta})$ is required depending on the problem. While MultiNest algorithm performs well with the relative error of 0.28%, the LLA-SS performs better, as the dimension of the parameter space is low, and gives a relative difference of only 0.14% in log evidence from the Monte Carlo estimate that uses 8 times as many likelihood evaluations. Similarly, the LLA-MCMC algorithm performs better than MultiNest, producing a relative difference of 0.11% in log evidence compared to a Monte Carlo sampling requiring nine times as many likelihood evaluations. Notably, both nested sampling and MultiNest require significantly more (30-45% more) function evaluations than, but without achieving comparable accuracy to, the proposed LLA-SS and LLA-MCMC methods. The estimated means and standard deviations of the parameters using the LLA-MCMC algorithm are shown in Table 5.

Next, a Bayesian model selection exercise is performed for this example to determine

Table 4: Comparison of evidence estimates using different algorithms for the second example, compared to conventional Monte Carlo and nested sampling.

Method	# fcn. eval.	$\log_e(\text{Evidence})$	Relative difference (%)
Monte Carlo	40,000	45.6407	—
Nested sampling	$\sim 8,000$	45.1889	0.99
MultiNest ($N_{\text{live}} = 1000$)	$\sim 7,000$	45.7676	0.28
LLA-IS	$\sim 6,500$	43.4989	4.69
LLA-SS	$\sim 4,900$	45.7038	0.14
LLA-MCMC	$\sim 4,400$	45.5899	0.11

Table 5: Posterior means and standard deviations of the parameters for the 11-story base isolated building (second example), computed using the LLA-MCMC algorithm.

Parameter	True value	Posterior Mean	Posterior Std. dev.
k_{post} (kN/m)	750	766.84	17.12
Q_y (% W)	5	5.04	0.25
r_k	0.1667	0.1677	0.0036

the restoring force model that best reproduces the measured data. The candidate models are Bouc-Wen, bilinear, and a linear approximation of the bilinear model according to the AASHTO (American Association of State Highway and Transportation Officials) guidelines. The bilinear model can be approximated by a Bouc-Wen model (35) as $n_{\text{pow}} \rightarrow \infty$; this

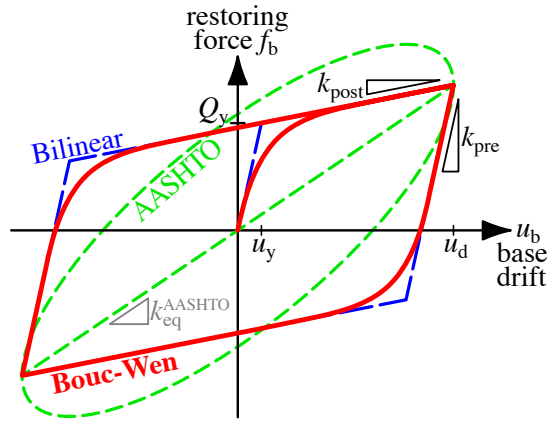


Figure 8: Models for isolator hysteresis.

study uses $n_{\text{pow}} = 100$, which is sufficiently large to produce a bilinear hysteresis loop. The AASHTO model approximates the energy dissipation in each cycle of the bilinear model,

approximating the isolator restoring force with

$$\begin{aligned} f_b &= c_{\text{eq}}\dot{u}_b + k_{\text{eq}}u_b \\ &= 2\zeta_{\text{eq}}\sqrt{k_{\text{eq}}(m_b + m_s)}\dot{u}_b + k_{\text{eq}}u_b. \end{aligned} \tag{37}$$

where m_s is the total mass of the superstructure (*i.e.*, $W = m_s g + m_b g$). The equivalent damping ratio ζ_{eq} and equivalent stiffness k_{eq} are given by

$$\begin{aligned} \zeta_{\text{eq}} &= \frac{2(1 - r_k)(1 - r_d^{-1})}{\pi[1 + r_k(r_d - 1)]} \\ k_{\text{eq}} &= \frac{k_{\text{pre}}}{r_d}[1 + r_k(r_d - 1)] \end{aligned} \tag{38}$$

where $r_d = u_d/u_y$ is the shear ductility ratio of the design displacement u_d to the yield displacement u_y .

The marginal likelihoods are calculated using the LLA-MCMC algorithm. With equal prior model probabilities, the posterior model probabilities are calculated using Bayes' theorem (1) and shown in Table 6. The model selection correctly assigns a posterior probability of 1.0 to Bouc-Wen model. Also note that, if the Bouc-Wen model is absent from the candidate model set, the Bayesian model selection chooses the second-best bilinear model as the correct one. This is expected because the bilinear model is the only remaining nonlinear model.

Table 6: Posterior model probabilities for the hysteretic isolation layer in the 11-DOF base-isolated building, estimated using the LLA-MCMC algorithm.

Model	$\log_e(\text{Evidence})$	$\mathbb{P}(\mathcal{M}_k \mathfrak{D})$
Bouc-Wen	45.6893	≈ 1.0
Bilinear	-46.1149	≈ 0.0
AASHTO	-821.0503	≈ 0.0

5.3. Example III: Flow past a cylinder

In this example, 2D fluid flow in a channel past a slightly off-center cylinder is considered, where the fluid inflow velocities are uncertain. Simulations are solved using the finite element method implemented in the FEniCS software package [66], adapted from one of the examples in its documentation. Figure 9 shows the cross-section of the channel of width $h = 0.41$ m and the cylinder of diameter 0.10 m.

The Navier-Stokes equation for an incompressible fluid, along with the mass conservation

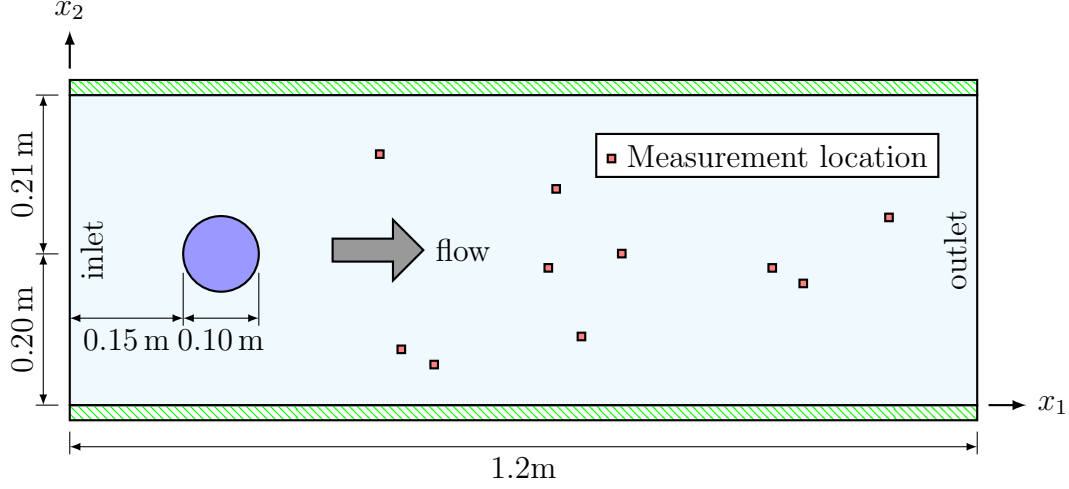


Figure 9: The setup for Example III where flow, with a parabolic velocity profile, enters the domain from left side. The measurement locations are shown using small squares.

equation, are

$$\begin{aligned} \frac{\partial \mathbf{u}}{\partial t} + (\mathbf{u} \cdot \nabla) \mathbf{u} &= -\frac{1}{\rho} \nabla p + \nu \nabla^2 \mathbf{u} \\ \nabla \cdot \mathbf{u} &= 0 \end{aligned} \quad (39)$$

where $\mathbf{u}(\mathbf{x}; t) = [u_1(\mathbf{x}; t), u_2(\mathbf{x}; t)]^T$ is the velocity vector at position $\mathbf{x} = [x_1, x_2]^T$; p is the pressure; ρ is the fluid density; ν is the kinematic viscosity of the fluid; and the gradient operator $\nabla = [\partial/\partial \mathbf{x}]^T = [\partial/\partial x_1, \partial/\partial x_2]^T$. Equations (39) are solved using the incremental pressure correction scheme in FEniCS. The inlet velocity profile is assumed parabolic

$$\mathbf{u}([0, x_2]^T; t, \theta) = \left[\frac{4x_2(h - x_2)}{h^2} \theta, 0 \right]^T \quad (40)$$

where θ is the uncertain peak inlet velocity. The velocity measurements are generated with $\theta_{\text{true}} = 1.2 \text{ m/s}$, which results in a flow with a Reynolds number of 80. The horizontal velocities are sampled at ten points $\mathbf{x}_1, \dots, \mathbf{x}_{10}$ randomly chosen downstream from the cylinder, starting at 1 s after the start of the flow and stopping before 1.6 s with an interval of 0.05 s, resulting in a total of $n = 120$ velocities $u_{1,l,k}^{\text{true}} = u_1(\mathbf{x}_l; t_k, \theta_{\text{true}})$, where $l = 1, \dots, 10$, $k = 1, \dots, 12$, and $t_k = 0.95 \text{ s} + (0.05 \text{ s})k$. These velocities are stacked into a vector and then corrupted by additive zero-mean Gaussian measurement noise

$$\mathbf{d} = \mathbf{d}_{\text{exact}} + \mathbf{v}, \quad \mathbf{d}_{\text{exact}} = [u_{1,1,1}^{\text{true}}, \dots, u_{1,1,12}^{\text{true}}, \dots, u_{1,10,1}^{\text{true}}, \dots, u_{1,10,12}^{\text{true}}]^T. \quad (41)$$

where the elements of \mathbf{v} are independent and identically distributed zero-mean Gaussian variables, each with a standard deviation that is 20% of the standard deviation of the 120 measurements — *i.e.*, 20% of $\{\mathbf{d}_{\text{exact}}^T \mathbf{d}_{\text{exact}} - [\frac{1}{10} \sum_{l=1}^{10} \frac{1}{12} \sum_{k=1}^{12} u_1(\mathbf{x}_l; t_k, \theta_{\text{true}})]^2\}^{1/2}$.

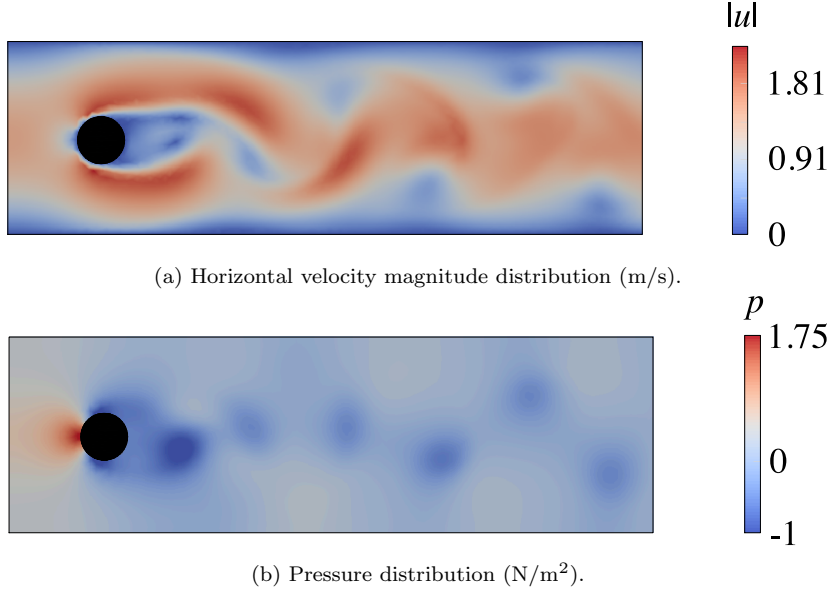


Figure 10: Typical velocity and pressure distributions in Example III at $t = 1.5$ s.

For prediction purposes, the measured velocity is assumed to contain both an additive measurement noise and a multiplicative modeling error. Herein, the multiplicative error is used as in Cheung *et al.* [67], Oliver and Moser [68], and Edeling *et al.* [69, 70]. In this uncertainty model, the measured velocity is assumed to be given by

$$u_1^{\text{meas}}(\mathbf{x}; t, \theta) = E_m(\mathbf{x})u_1(\mathbf{x}; t, \theta) + e \quad (42)$$

where $u_1(\mathbf{x}; t, \theta)$ is the velocity obtained by solving (39); the multiplicative modeling error given by $E_m(\mathbf{x})$ is used to generate the modeling uncertainty; and e is the measurement error. The required covariances are then written as

$$k_{uu}(\mathbf{x}, \mathbf{x}'; t|\theta) = u_1(\mathbf{x}; t, \theta)k_{E_m}(\mathbf{x}, \mathbf{x}'; t|\theta)u_1(\mathbf{x}'; t, \theta) \quad (43)$$

where the measurement error is assumed independent. The multiplicative error E_m is assumed herein to be a time-invariant, spatial Gaussian process with unit mean and covariance function given by

$$k_{E_m}(\mathbf{x}, \mathbf{x}'; t|\boldsymbol{\theta}_{\text{hyp}}) = \sigma^2 \exp \left[-\sum_{i=1}^2 \left(\frac{x_i - x'_i}{l_i} \right)^2 \right] \quad (44)$$

where the hyperparameters are $\boldsymbol{\theta}_{\text{hyp}} = [\sigma, l_1, l_2]^T$. The measurement errors in \mathbf{d} are assumed distributed as $\mathcal{N}(\mathbf{0}, \boldsymbol{\Sigma}_e)$, where $\boldsymbol{\Sigma}_e = \sigma_e \mathbf{I}$ is a diagonal matrix. A Gaussian likelihood function is constructed, next, as

$$p(\mathfrak{D}|\theta) = \frac{1}{(2\pi)^{n/2} |\boldsymbol{\Sigma}|^{1/2}} \exp \left\{ -\frac{1}{2} [\mathbf{u}_1(\theta) - \mathbf{d}]^T \boldsymbol{\Sigma}^{-1} [\mathbf{u}_1(\theta) - \mathbf{d}] \right\} \quad (45)$$

where $\mathbf{u}_1(\theta) = [u_{1,1,1}^\theta, \dots, u_{1,1,12}^\theta, \dots, u_{1,10,1}^\theta, \dots, u_{1,10,12}^\theta]^\top$, and $u_{1,l,k}^\theta \equiv u_1(\mathbf{x}_l; t_k, \theta)$. consists of the 120 velocities predicted using parameter θ corresponding to each element in \mathbf{d} ; $\Sigma = \Sigma_e + \Sigma_{E_m}$ is the covariance matrix of the likelihood, where Σ_{E_m} is formed using the covariance of the Gaussian process E_m in (44), *i.e.*, where the $(p + 12[j - 1], q + 12[k - 1])$ element of Σ_{E_m} is

$$\sigma^2 u_1(\mathbf{x}_j; t_p) u_1(\mathbf{x}_k; t_q) \left/ \prod_{i=1}^2 \exp\left(\frac{x_{j,i} - x_{k,i}}{l_i}\right)^2 \right. \quad (46)$$

for $j, k = 1, \dots, 10$ and $p, q = 1, \dots, 12$. The hyperparameters are assumed here as $\sigma = 0.2\sqrt{\text{Var}(\mathbf{d})}$, and $l_1 = l_2 = 1$ m to model the correlated and corrupted measurement data. The prior for peak inlet velocity θ is assumed to be a truncated Gaussian with mean 1.25 m/s and standard deviation 0.5 m/s, truncated at 1.0 and 1.5 m/s.

The LLA-IS algorithm is implemented with a truncated Gaussian importance density formed at each iteration, using the mean of the current samples and a standard deviation of 0.25 m/s, truncated at 1.0 and 1.5 m/s, and with $\gamma_S = 0.5N$ and an initial sample size of $N = 25$. The likelihood levels are decided at iteration i based on the fraction $f_i^{\text{reject}} = \min(0.5, 0.1 + 0.025(i - 1))$. The LLA-SS algorithm is implemented again with $\Theta^{(s)} = \left\{ F_\theta^{-1}(\theta) \mid \theta \in \left(\frac{s-1}{n_{\text{st}}}, \frac{s}{n_{\text{st}}} \right) \right\}$, where $n_{\text{st}} = 5$, and F_θ is the probability distribution of the peak inlet velocity θ ; for this algorithm, the likelihood levels are decided at every iteration based on the fraction $f_i^{\text{reject}} = 0.25$. The LLA-MCMC algorithm is implemented with an initial sample size of 100 and, at each iteration, the 20 samples with the lowest likelihoods are rejected. 20 new samples with likelihoods larger than the highest likelihood value of the rejected samples are added to the sample pool using the Metropolis-Hastings algorithm with a proposal density that is a truncated Gaussian with a standard deviation 0.1 m/s and truncated at 1 m/s and 1.5 m/s. The stopping criteria are the same as in Example I except $\Delta\mathcal{E}_{\text{tol}} = 1\%$ and a maximum of 5000 likelihood evaluations.

The accuracies of the proposed algorithms, again compared to Monte Carlo and nested sampling, are shown in Table 7. The sufficient number of likelihood function evaluations for the Monte Carlo approach is estimated similar to Example II. All three algorithms give small relative difference in the log evidence here as shown in Table 7. The LLA-SS performs well, as the dimension of the parameter space is low. The LLA-IS and LLA-MCMC algorithms in this example also produce small relative differences compared to Monte Carlo sampling with 5.7 times as many likelihood evaluations. When compared to nested sampling with similar numbers of likelihood evaluations, the proposed algorithms — notably LLA-MCMC — show improved accuracy almost up to two orders of magnitude.

5.4. Example IV: Steady state heat conduction within an inhomogeneous plate

This example explores the LLA-MCMC algorithm on a high-dimensional problem, for which it is more suited than the other two algorithms that may suffer significantly from the curse of dimensionality, as discussed in Section 3. In particular, finding a good importance density for LLA-IS method in high-dimension is difficult resulting in inefficient sampling from the high-likelihood region, and the total number of strata for LLA-SS, $\bar{n}_{\text{st}} = (n_{\text{st}})^{n_\theta}$, increases exponentially. Although, a good rejection algorithm like MultiNest is efficient

Table 7: Comparison of evidence estimates, using different algorithms for the third example, compared to conventional Monte Carlo and nested sampling.

Method	# fcn. eval	$\log_e(\text{Evidence})$	Relative difference (%)
Monte Carlo	20,000	252.5201	—
Nested sampling	$\sim 4,000$	252.2854	0.0929
LLA-IS	$\sim 3,500$	252.5498	0.0118
LLA-SS	$\sim 3,500$	252.5067	0.0053
LLA-MCMC	$\sim 3,500$	252.5249	0.0019

in low dimensions, an exponential scaling emerges in higher dimensions [71] because the volume of the parameter space expands exponentially with the number of dimensions, and the number of active points must be increased to obtain accurate estimates [45].

A square thin plate of dimension $2\text{ m} \times 2\text{ m}$ is composed of an inhomogeneous material with a coordinate system origin at its center. One edge (at $y = -1\text{ m}$) is subjected to a fixed temperature of 100°C ; the other three edges are thermally insulated. A point source of $Q = 25\text{ W}$ is located in the interior at $x = -0.5\text{ m}$, $y = 0$. The material thermal conductivity $k(x_1, x_2) = k_0 \exp[z(x_1, x_2)]$ is assumed uncertain, where $z(x_1, x_2)$ is an underlying unitless zero-mean Gaussian field and, herein, $k_0 = 1\text{ W}/(\text{m}^2 \cdot \text{K})$. To keep the problem simple, the covariance kernel of the latent field is assumed as

$$\mathbb{E}[z(x_1, x_2)z(y_1, y_2)] = \sigma^2 \exp\left(\sum_{i=1}^2 -\frac{|x_i - y_i|}{l_i}\right) \quad (47)$$

where l_1 and l_2 are the correlation lengths and $\sigma = 1.5$ is used. Next, the latent random field $z(x_1, x_2)$ is expressed using a Karhunen-Loève expansion truncated at the M th term:

$$z(x_1, x_2) = \sum_{i=1}^M \omega_i \xi_i f_i(x_1, x_2) \quad (48)$$

where the ω_i^2 and $f_i(x_1, x_2)$ are the eigenvalues and eigenfunctions, respectively, of the covariance kernel; the ξ_i are standard unit normal variables; $M = 100$ is selected to capture 99.6% of total energy. Hence, the dimension of the uncertain parameter vector is 100 in this example. To generate the temperature measurements in the steady-state condition, correlation lengths $l_1 = l_2 = 0.75\text{ m}$ are used; 25 random points are selected on the plate, at which temperatures are measured and corrupted by 10% Gaussian additive sensor noise (*i.e.*, the noises at the sensors are independent and identically distributed zero-mean Gaussian random variables with a standard deviation that is 10% of the standard deviation of the noise-free measurements. A typical temperature distribution is shown in Figure 11.

Using a Gaussian likelihood and guessing the correlation lengths both to (incorrectly) be 1.0 m , the marginal likelihood is estimated with an initial sample size of 100 using the LLA-MCMC algorithm. The stopping criterion is solely that the change in evidence be

smaller than 0.1%. The result is compared in Table 8 to Monte Carlo sampling with 6×10^5 likelihood evaluations to a nested sampling algorithm that is run to the same level of $\hat{\chi}_{\text{final}}^{\text{MCMC}}$. The sufficient number of likelihood function evaluations for the Monte Carlo approach is estimated similar to Example II. LLA-MCMC again provides better accuracy compared to nested sampling using only two-thirds as many likelihood evaluations.

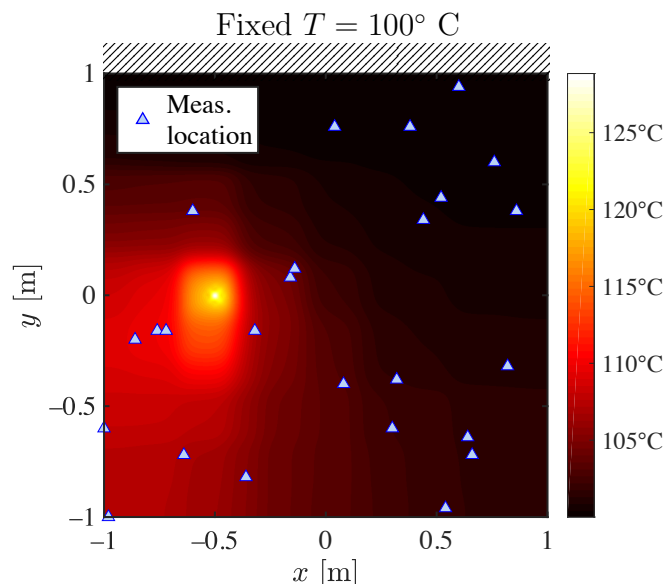


Figure 11: Typical temperature distribution with 25 random measurement locations shown.

Table 8: Comparison of evidence estimate using LLA-MCMC algorithm for Example IV, compared to conventional Monte Carlo and nested sampling.

Method	# fcn. eval.	$\log_e(\text{Evidence})$	Relative difference (%)
Monte Carlo	60×10^4	-30.2160	—
Nested sampling	$\sim 12 \times 10^4$	-31.1172	2.98
LLA-MCMC	$\sim 8 \times 10^4$	-30.1295	0.29

A model selection problem is also implemented for this example, where each model is a polynomial chaos expansion (PCE) [72] of different orders. However, the number of terms in the Karhunen-Loève expansion is limited to $M = 22$ to capture 92% of total energy. Bayesian model selection is performed to evaluate the suitability of second-order, third-order, and sparse fourth-order PCEs with Hermite polynomials. For the second and third PCEs, an ordinary least-squares minimization is used to estimate the coefficients. A least angle regression is used for estimation of the coefficients of the sparse fourth-order PCE [73]. The result, reported in Table 9, shows that a third-order PCE is better than second-order in this example. However, a fourth-order sparse PCE performs poorly compared to any second- or third-order expansions.

Table 9: Posterior model probabilities for different orders of polynomial chaos expansion.

PCE order	$\log_e(\text{Evidence})$	$\mathbb{P}(\mathcal{M}_k \mathfrak{D})$
second	-36.1309	0.31
third	-35.3233	0.69
fourth (Sparse)	-51.6090	0.00

6. Conclusions

A likelihood level adapted approach has been proposed herein to evaluate the multi-dimensional integral known as the marginal likelihood, or evidence, that is required in Bayesian model selection. Three algorithms using importance sampling, stratified sampling, and Markov chain Monte Carlo are used to implement this approach, and compared with Monte Carlo and two nested sampling algorithms (original and MultiNest). In the first proposed algorithm (LLA-IS), importance sampling densities are formed adaptively at each iteration of the algorithm to generate samples with increased levels of likelihood; the performance of this algorithm depends, however, on the effectiveness of the assumed importance sampling density and, as a result, LLA-IS can become inefficient in sampling from high-likelihood regions. The second algorithm (LLA-SS) uses stratified sampling and focuses on generating more samples from the strata with higher likelihoods. This algorithm is the most accurate method for models with complicated behavior in low dimension. It can also be implemented in parallel for each stratum. However, this algorithm can suffer from the curse of dimensionality for problems with high-dimensional parameter spaces. The final algorithm (LLA-MCMC) uses Markov chain Monte Carlo algorithms to sample more from the high likelihood region; for high-dimensional parameter spaces, MCMC algorithms with high acceptance rates, *e.g.*, the modified Metropolis-Hastings algorithm [56], can be used.

The performance and accuracy of these proposed algorithms are compared in four numerical examples. The first example shows the accuracy of the proposed algorithms for a problem with a known marginal likelihood. The second example evaluates the marginal likelihood (evidence) for a model where the underlying physics requires many solution of the Navier-Stokes equations; the proposed algorithms are shown to give results that are within the desired accuracy level relative to those estimated using the well-known nested sampling algorithm. The third example uses an 11-story base-isolated building model, with uncertainties in the nonlinear hysteretic isolation layer, subjected to a historical earthquake; the uncertain isolation-layer parameters provide a multidimensional parameter space. The fourth example involves heat conduction in a plate with uncertain thermal conductivity, which is modeled as a random field with 100 stochastic dimensions. The LLA-MCMC algorithm applied to this problem shows the accuracy of the proposed algorithm when multi-dimensional uncertainty is present. These examples show the efficacy of the proposed algorithms in different settings and their application to Bayesian model selection. The LLA-IS algorithm, however, needs a better selection strategy to construct the importance sampling densities. Similarly, the application of sparse quadrature to the LLA-SS algorithm needs to be in-

vestigated. In future, the proposed algorithms will also be implemented for multi-physics problems, and their efficient parallel implementation will be explored.

Appendix A. The stochastic error ϵ_s

The stochastic error is defined as

$$\sum_{i=0}^{i_{\text{final}}} \lambda_i [\Delta\chi(\lambda_i) - \Delta\widehat{\chi}_i] = \sum_{i=0}^{i_{\text{final}}} \lambda_i \epsilon_{s,i} \quad (\text{A.1})$$

where each component of the error is $\epsilon_{s,i} = \Delta\chi(\lambda_i) - \Delta\widehat{\chi}_i$.

Proposition 1. *For each i , the stochastic error component, $\Delta\widehat{\chi}_i$ converges to $\Delta\chi(\lambda_i)$, and its coefficient of variation (COV) is $\mathcal{O}(N^{-1/2})$ when the samples are uncorrelated and N , the number of samples, is large.*

Proof. For a large number N of samples, using the strong law of large numbers, $\Delta\widehat{\chi}_i$ converges to $\Delta\chi(\lambda_i)$ almost surely [74] as the mean of a sequence of random variables. Hence, $\epsilon_{s,i} = \lambda_i[\Delta\chi(\lambda_i) - \Delta\widehat{\chi}_i]$ is zero-mean for large N . Further, denote $\mathbb{I}_{i,k}(\boldsymbol{\theta}_j) = \mathbb{I}_{\widetilde{\Theta}_i}(\boldsymbol{\theta}_j) [1 - \mathbb{I}_{\widetilde{\Theta}_k}(\boldsymbol{\theta}_j)]$, *i.e.*, an indicator that sample $\boldsymbol{\theta}_j$ is in $\widetilde{\Theta}_i$ but outside $\widetilde{\Theta}_k$. Hence,

$$\Delta\widehat{\chi}_i = \frac{1}{N} \sum_{j=1}^N \mathbb{I}_{i-1,i}(\boldsymbol{\theta}_j) \quad (\text{A.2})$$

and

$$\begin{aligned} \mathbb{E}[(\Delta\widehat{\chi}_i - \Delta\chi(\lambda_i))^2] &= \mathbb{E}\left[\left(\frac{1}{N} \sum_{j=1}^N [\mathbb{I}_{i-1,i}(\boldsymbol{\theta}_j) - \Delta\chi(\lambda_i)]\right)^2\right] \\ &= \frac{1}{N^2} \sum_{j=1}^N \sum_{l=1}^N \mathbb{E}\left[(\mathbb{I}_{i-1,i}(\boldsymbol{\theta}_j) - \Delta\chi(\lambda_i))(\mathbb{I}_{i-1,i}(\boldsymbol{\theta}_l) - \Delta\chi(\lambda_i))\right] \end{aligned} \quad (\text{A.3})$$

Note that the $\mathbb{I}_{i-1,i}(\boldsymbol{\theta}_j)$ are Bernoulli random variables with success probabilities $\Delta\chi(\lambda_i)$. Assume the samples are uncorrelated, *i.e.*,

$$\begin{aligned} \mathbb{E}\left[(\mathbb{I}_{i-1,i}(\boldsymbol{\theta}_j) - \Delta\chi(\lambda_i))(\mathbb{I}_{i-1,i}(\boldsymbol{\theta}_l) - \Delta\chi(\lambda_i))\right] &= 0 \quad \text{for } j \neq l \\ \mathbb{E}\left[(\mathbb{I}_{i-1,i}(\boldsymbol{\theta}_j) - \Delta\chi(\lambda_i))^2\right] &= \text{Var}(\mathbb{I}_{i-1,i}(\boldsymbol{\theta}_j)) \\ &= \Delta\chi(\lambda_i) [1 - \Delta\chi(\lambda_i)] \end{aligned} \quad (\text{A.4})$$

Using these relations,

$$\begin{aligned}\text{Var}(\Delta\hat{\chi}_i) &= \frac{\Delta\chi(\lambda_i)[1 - \Delta\chi(\lambda_i)]}{N} \\ \text{COV}(\Delta\hat{\chi}_i) &= \sqrt{\frac{1 - \Delta\chi(\lambda_i)}{N\Delta\chi(\lambda_i)}}\end{aligned}\tag{A.5}$$

References

- [1] Y. Sakamoto, M. Ishiguro, G. Kitagawa, Akaike information criterion statistics, Dordrecht, The Netherlands: D. Reidel 81 (10.5555) (1986) 26853.
- [2] G. Schwarz, et al., Estimating the dimension of a model, *The Annals of Statistics* 6 (2) (1978) 461–464.
- [3] G. Claeskens, N. L. Hjort, The focused information criterion, *Journal of the American Statistical Association* 98 (464) (2003) 900–916.
- [4] P. Grünwald, T. Roos, Minimum description length revisited, *Int. J. Math. Ind.* 11 (01) (2019) 1930001.
- [5] D. J. Spiegelhalter, N. G. Best, B. P. Carlin, A. Linde, The deviance information criterion: 12 years on, *J. R. Stat. Soc. Ser. B. Stat. Methodol.* 76 (3) (2014) 485–493.
- [6] K. Popper, *The logic of scientific discovery*, Routledge, 2005.
- [7] S. De, P. T. Brewick, E. A. Johnson, S. F. Wojtkiewicz, Investigation of model falsification using error and likelihood bounds with application to a structural system, *Journal of Engineering Mechanics* 144 (9) (2018) 04018078.
- [8] K. P. Burnham, D. R. Anderson, *Model selection and multimodel inference: a practical information-theoretic approach*, Springer Science & Business Media, 2002.
- [9] A. Dasgupta, E. A. Johnson, Model falsification from a Bayesian viewpoint with applications to parameter inference and model selection of dynamical systems, *Journal of Engineering Mechanics* 150 (6) (2024) 04024023.
- [10] S. De, E. A. Johnson, S. F. Wojtkiewicz, P. T. Brewick, Computationally efficient Bayesian model selection for locally nonlinear structural dynamic systems, *Journal of Engineering Mechanics* 144 (5) (2018) 04018022.
- [11] S. De, P. T. Brewick, E. A. Johnson, S. F. Wojtkiewicz, A hybrid probabilistic framework for model validation with application to structural dynamics modeling, *Mechanical Systems and Signal Processing* 121 (2019) 961–980.
- [12] C. Rao, Y. Wu, S. Konishi, R. Mukerjee, *On model selection*, Lecture Notes-Monograph Series (2001) 1–64.
- [13] H. Chipman, E. I. George, R. E. McCulloch, M. Clyde, D. P. Foster, R. A. Stine, *The practical implementation of Bayesian model selection*, Lecture Notes-Monograph Series (2001) 65–134.
- [14] K. M. Cremers, Stock return predictability: A Bayesian model selection perspective, *Review of Financial Studies* 15 (4) (2002) 1223–1249.
- [15] W. L. Crouse, G. R. Keele, M. S. Gastonguay, G. A. Churchill, W. Valdar, A Bayesian model selection approach to mediation analysis, *PLOS Genetics* 18 (5) (2022) 1–33.
- [16] C. Andrieu, P. Djurić, A. Doucet, Model selection by MCMC computation, *Signal Processing* 81 (1) (2001) 19–37.
- [17] J. L. Beck, K.-V. Yuen, Model selection using response measurements: Bayesian probabilistic approach, *Journal of Engineering Mechanics* 130 (2) (2004) 192–203.
- [18] J. L. Beck, Bayesian system identification based on probability logic, *Structural Control and Health Monitoring* 17 (7) (2010) 825–847.
- [19] S. H. Cheung, J. L. Beck, Calculation of posterior probabilities for Bayesian model class assessment and averaging from posterior samples based on dynamic system data, *Computer-Aided Civil and Infrastructure Engineering* 25 (5) (2010) 304–321.

- [20] M. Muto, J. L. Beck, Bayesian updating and model class selection for hysteretic structural models using stochastic simulation, *Journal of Vibration and Control* 14 (1-2) (2008) 7–34.
- [21] L. Mthembu, T. Marwala, M. I. Friswell, S. Adhikari, Model selection in finite element model updating using the Bayesian evidence statistic, *Mech. Syst. Signal Pr.* 25 (7) (2011) 2399–2412.
- [22] E. T. Jaynes, *Probability Theory: The Logic of Science*, Cambridge University Press, Cambridge, U.K., 2003.
- [23] R. E. Kass, A. E. Raftery, Bayes factors, *J. Amer. Statist. Assoc.* 90 (430) (1995) 773–795.
- [24] S. N. Goodman, Toward evidence-based medical statistics. 2: The Bayes factor, *Annals of internal medicine* 130 (12) (1999) 1005–1013.
- [25] D. J. C. MacKay, Bayesian interpolation, *Neural Computation* 4 (3) (1992) 415–447.
- [26] D. J. C. MacKay, *Bayesian methods for adaptive models*, Ph.D. thesis, California Institute of Technology (1992).
- [27] S. F. Gull, Bayesian inductive inference and maximum entropy, in: *Maximum-entropy and Bayesian methods in science and engineering*, Springer, 1988, pp. 53–74.
- [28] M. A. Newton, A. E. Raftery, Approximate Bayesian inference with the weighted likelihood bootstrap, *Journal of the Royal Statistical Society. Series B (Methodological)* 56 (1) (1994) 3–48.
- [29] A. E. Raftery, M. A. Newton, J. M. Satagopan, P. N. Krivitsky, Estimating the integrated likelihood via posterior simulation using the harmonic mean identity, in: J. M. Bernardo, M. J. Bayarri, J. O. Berger, A. P. Dawid, D. Heckerman, A. F. M. Smith, M. West (Eds.), *Bayesian Statistics 8: Proceedings of the Eighth Valencia International Meeting*, Oxford University Press, Oxford, 2004, pp. 1–45.
- [30] M.-N. Tran, M. Scharth, D. Gunawan, R. Kohn, S. D. Brown, G. E. Hawkins, Robustly estimating the marginal likelihood for cognitive models via importance sampling, *Behavior Research Methods* 53 (3) (2021) 1148–1165.
- [31] M. F. Bugallo, V. Elvira, L. Martino, D. Luengo, J. Miguez, P. M. Djuric, Adaptive importance sampling: The past, the present, and the future, *IEEE Signal Processing Magazine* 34 (4) (2017) 60–79.
- [32] I. Schuster, I. Klebanov, Markov chain importance sampling—a highly efficient estimator for mcmc, *Journal of Computational and Graphical Statistics* 30 (2018) 260 – 268.
- [33] R. M. Neal, Annealed importance sampling, *Stat. Comput.* 11 (2) (2001) 125–139.
- [34] Y. Li, N. Wang, J. Yu, Improved marginal likelihood estimation via power posteriors and importance sampling, *Journal of Econometrics* 234 (1) (2023) 28–52.
- [35] N. Friel, A. N. Pettitt, Marginal likelihood estimation via power posteriors, *J. R. Stat. Soc. Ser. B Stat. Methodol.* 70 (3) (2008) 589–607.
- [36] J. Ching, Y.-C. Chen, Transitional Markov chain Monte Carlo method for Bayesian model updating, model class selection, and model averaging, *J. Eng. Mech.* 133 (7) (2007) 816–832.
- [37] Z. I. Botev, D. P. Kroese, Efficient Monte Carlo simulation via the generalized splitting method, *Statistics and Computing* 22 (1) (2012) 1–16.
- [38] M. Chiachio, J. L. Beck, J. Chiachio, G. Rus, Approximate Bayesian computation by subset simulation, *SIAM Journal on Scientific Computing* 36 (3) (2014) A1339–A1358.
- [39] F. A. DiazDelaO, A. Garbuno-Inigo, S. K. Au, I. Yoshida, Bayesian updating and model class selection with subset simulation, *Computer Methods in Applied Mechanics and Engineering* 317 (2017) 1102 – 1121.
- [40] M. K. Vakilzadeh, Y. Huang, J. L. Beck, T. Abrahamsson, Approximate Bayesian computation by subset simulation using hierarchical state-space models, *Mechanical Systems and Signal Processing* 84 (2017) 2 – 20.
- [41] J. B. Nagel, B. Sudret, Spectral likelihood expansions for Bayesian inference, *Journal of Computational Physics* 309 (2016) 267–294.
- [42] J. Skilling, Nested sampling for general Bayesian computation, *Bayesian Analysis* 1 (4) (2006) 833–859.
- [43] F. Feroz, M. P. Hobson, M. Bridges, MultiNest: an efficient and robust bayesian inference tool for cosmology and particle physics, *Monthly Notices of the Royal Astronomical Society* 398 (4) (2009) 1601–1614.

- [44] A. J. Dittmann, Notes on the practical application of nested sampling: Multinest, (non)convergence, and rectification, arXiv preprint arXiv:2404.16928 (2024).
- [45] F. Feroz, M. Hobson, E. Cameron, A. Pettitt, Importance nested sampling and the MultiNest algorithm, *The Open Journal of Astrophysics* 2 (Jun. 2013).
- [46] N. G. Polson, J. G. Scott, Vertical-likelihood Monte Carlo, arXiv preprint arXiv:1409.3601 (2014).
- [47] F. Llorente, L. Martino, D. Delgado, J. López-Santiago, Marginal likelihood computation for model selection and hypothesis testing: An extensive review, *SIAM Review* 65 (1) (2023) 3–58.
- [48] J. Shaw, M. Bridges, M. Hobson, Efficient bayesian inference for multimodal problems in cosmology, *Monthly Notices of the Royal Astronomical Society* 378 (4) (2007) 1365–1370.
- [49] F. Feroz, M. P. Hobson, Multimodal nested sampling: an efficient and robust alternative to Markov Chain Monte Carlo methods for astronomical data analyses, *Monthly Not., Royal Astro. Soc.* 384 (2) (2008) 449–463.
- [50] S. M. Ross, *Simulation*, 5th Edition, Academic Press, 2013.
- [51] M. D. McKay, R. J. Beckman, W. J. Conover, Comparison of three methods for selecting values of input variables in the analysis of output from a computer code, *Technometrics* 21 (2) (1979) 239–245.
- [52] S. Chib, E. Greenberg, Understanding the Metropolis-Hastings algorithm, *The American Statistician* 49 (4) (1995) 327–335.
- [53] S. Chib, Markov chain Monte Carlo methods: computation and inference, in: *Handbook of Econometrics*, Vol. 5, Elsevier, 2001, pp. 3569–3649.
- [54] C. Andrieu, N. De Freitas, A. Doucet, M. I. Jordan, An introduction to MCMC for machine learning, *Machine Learning* 50 (1) (2003) 5–43.
- [55] L. Tierney, Markov chains for exploring posterior distributions, *The Annals of Statistics* (1994) 1701–1728.
- [56] S.-K. Au, J. L. Beck, Estimation of small failure probabilities in high dimensions by subset simulation, *Probabilistic Engineering Mechanics* 16 (4) (2001) 263–277.
- [57] P. Mukherjee, D. Parkinson, A. R. Liddle, A nested sampling algorithm for cosmological model selection, *The Astrophysical Journal Letters* 638 (2) (2006) L51–L54.
- [58] P. Del Moral, J. Garnier, Genealogical particle analysis of rare events, *The Annals of Applied Probability* 15 (4) (2005) 2496–2534.
- [59] F. Cérou, P. Del Moral, T. Furon, A. Guyader, Sequential Monte Carlo for rare event estimation, *Statistics and Computing* 22 (3) (2012) 795–808.
- [60] N. Chopin, C. P. Robert, Properties of nested sampling, *Biometrika* 97 (3) (2010) 741–755.
- [61] K. Łatuszyński, M. T. Moores, T. Stumpf-Fétizon, MCMC for multi-modal distributions, arXiv preprint arXiv:2501.05908 (2025).
- [62] K. P. Murphy, *Conjugate Bayesian analysis of the Gaussian distribution*.
- [63] M. Kamalzare, E. A. Johnson, S. F. Wojtkiewicz, Computationally efficient design of optimal output feedback strategies for controllable passive damping devices, *Smart Materials and Structures* 23 (5) (2014) 055027.
- [64] Y.-K. Wen, Method for random vibration of hysteretic systems, *J. Eng. Mech. Div. ASCE* 102 (2) (1976) 249–263.
- [65] R. I. Skinner, W. H. Robinson, G. H. McVerry, *An Introduction to Seismic Isolation*, Wiley, Chichester, 1993.
- [66] H. P. Langtangen, A. Logg, *Solving PDEs in Python: the FEniCS tutorial I*, Springer, 2016.
- [67] S. H. Cheung, T. A. Oliver, E. E. Prudencio, S. Prudhomme, R. D. Moser, Bayesian uncertainty analysis with applications to turbulence modeling, *Reliability Engineering & System Safety* 96 (9) (2011) 1137–1149.
- [68] T. A. Oliver, R. D. Moser, Bayesian uncertainty quantification applied to RANS turbulence models, in: *Journal of Physics: Conference Series*, Vol. 318, IOP Publishing, 2011, p. 042032.
- [69] W. Edeling, P. Cinnella, R. P. Dwight, H. Bijl, Bayesian estimates of parameter variability in the $k-\epsilon$ turbulence model, *Journal of Computational Physics* 258 (2014) 73–94.
- [70] W. Edeling, P. Cinnella, R. P. Dwight, Predictive RANS simulations via Bayesian model-scenario

- averaging, *Journal of Computational Physics* 275 (2014) 65–91.
- [71] W. J. Handley, M. P. Hobson, A. N. Lasenby, polychord: nested sampling for cosmology, *Monthly Notices of the Royal Astronomical Society: Letters* 450 (1) (2015) L61–L65.
 - [72] R. G. Ghanem, P. D. Spanos, Stochastic finite element method: Response statistics, in: *Stochastic Finite Elements: A Spectral Approach*, Springer, 1991, pp. 101–119.
 - [73] B. Efron, T. Hastie, I. Johnstone, R. Tibshirani, Least angle regression, *The Annals of Statistics* 32 (2) (2004) 407–499.
 - [74] W. Feller, *An introduction to probability theory and its applications*, Vol. 1, John Wiley & Sons, 2008.